Unit 7 Quantum Oscillators

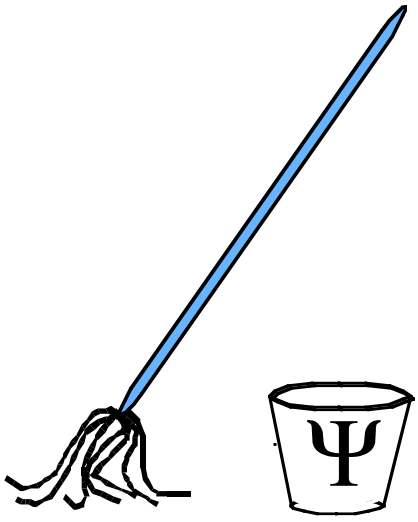

Chapter 21

Two-Dimensional Oscillator States and Dynamics

W. G. Harter

Using the 1D-harmonic oscillator algebra from the preceding Chapter 20, the 2D oscillator quantum mechanics is developed. Much of the theory applies to 3D, 4D, and higher dimensional oscillators, as well. Quantum em fields treated in Chapter 22 begin with many-D oscillators, one dimension for each em-mode. However, the main objective of this Chapter 21 is to give the quantum version of the classical ABCD oscillator analogy to quantum spin-1/2, polarization, and other U(2) systems discussed in Chapter 10. This sets the stage for a powerful development, due to Schwinger, of the quantum theory of angular momentum in Chapter 23.

CHAPTER 21. 2D-HARMONIC OSCILLATOR STATES AND DYNAMICS 1

Chapter 21. 2D-Harmonic Oscillator States and Dynamics

21.1 Two-Dimensional Harmonic Oscillator Hamiltonians and Bases

So far, most wavefunctions have been one-dimensional . The classical waves in the "Hall of Mirrors" wave-guide and its cavity described in Sec. 6.3 are one exception. Now we extend the oscillator theory of the preceding Chapter 20 to an oscillator system of two (or more) dimensions.

(a) 2D-Oscillator basics

As far as symmetry algebra goes it is a big jump to go from a 1D oscillator Hamiltonian with a *U(1)* phase space (The 1-D phase space has to two real dimensions *(x,p)* or one complex dimension $\alpha=x+ip$) to a 2D oscillator with a *U(2)* phase space. The 2-D oscillator phase space has four real *phase space* dimensions (x_1, p_1, x_2, p_2) or two complex *phasor* dimensions ($\alpha_1 = x_1+ip_1$, $\alpha_2 = x_2+ip_2$).

To help understand the physics and mathematics of this formidable system it helps to appeal to the analogy in Sec. 10.1 between a two-dimensional classical oscillator and a two state quantum system. The *U(2)* catalog in Fig. 10.4.2 showed three archetypes of 2-state Hamiltonians labeled *A*, *B*, and *C* each corresponding to different values of parameters *A*, *B*, *C*, and *D* that give different symmetry and physics. The goal here is to solve (and more importantly, understand) the eigensolutions of the quantum version of the *A*, *B*, and *C* type oscillators and how their solutions are derived as symmetry varies.

(1) Hamiltonians and operators

The first step is easy. We rewrite a classical 2-D Hamiltonian (10.1.3a) with a thick-tip pen!

$$\mathbf{H} = \frac{A}{2}\left(\mathbf{p}_1^2 + \mathbf{x}_1^2\right) + B\left(\mathbf{x}_1\mathbf{x}_2 + \mathbf{p}_1\mathbf{p}_2\right) + C\left(\mathbf{x}_1\mathbf{p}_2 - \mathbf{x}_2\mathbf{p}_1\right) + \frac{D}{2}\left(\mathbf{p}_2^2 + \mathbf{x}_2^2\right) \qquad (21.1.1)$$

The second step is not so hard either. The symmetric form lets us relate each **x** and **p** to creation and destruction operators as in (20.2.1) and (20.2.16). (Here the pesky $\sqrt{M}$ and $\hbar$ factors are absorbed in *A, B, C*, and *D*.) Each oscillator dimension has a set of operators. First, the number-1 oscillator is set up.

$$\mathbf{a}_1 = (\mathbf{x}_1 + i\,\mathbf{p}_1)/\sqrt{2} \qquad \mathbf{a}^\dagger_1 = (\mathbf{x}_1 - i\,\mathbf{p}_1)/\sqrt{2} \qquad (21.1.2a)$$

$$\mathbf{x}_1 = (\mathbf{a}^\dagger_1 + \mathbf{a}_1)/\sqrt{2} \qquad \mathbf{p}_1 = i\,(\mathbf{a}^\dagger_1 - \mathbf{a}_1)/\sqrt{2} \qquad (21.1.2b$$

Then, the number-2 oscillator gets the same treatment.

$$\mathbf{a}_2 = (\mathbf{x}_2 + i\,\mathbf{p}_2)/\sqrt{2} \qquad \mathbf{a}^\dagger_2 = (\mathbf{x}_2 - i\,\mathbf{p}_2)/\sqrt{2} \qquad (21.1.2c)$$

$$\mathbf{x}_2 = (\mathbf{a}^\dagger_2 + \mathbf{a}_2)/\sqrt{2} \qquad \mathbf{p}_2 = i\,(\mathbf{a}^\dagger_2 - \mathbf{a}_2)/\sqrt{2} \qquad (21.1.2d)$$

(2) Commutation relations: Bosons and Fermions

The next step involves a little thinking about what sort of commutation relations these operators should obey. It helps to think about what a 2-D oscillator model would model in the real world. Perhaps, the thing that comes to mind is a particle in a 2-D harmonic potential as was shown in Fig. 10.1.2. As

explained in Appendix 10.A-B, this is also a model for optical polarization described in $(x, y) = (x_1, x_2)$ space or a charged particle in a very cold magnetic or optical trap.

However, as shown by Fig. 10.1.1 a-b, a 2D oscillator is also a model for two 1D oscillators that may or may not be coupled to each other. In other words, a 2D oscillator could be a two-particle system with particle-1 and particle-2 each having a separate 1D coordinate x_1, and x_2, respectively.

Different dimensions for any system are orthogonal and independent. Either can be transformed without affecting the other. For this reason we will demand *inter-dimensional commutivity*.

$$[\,\mathbf{x}_1\,,\mathbf{p}_2] = \mathbf{0} = [\,\mathbf{x}_2\,,\mathbf{p}_1]\,,\quad [\,\mathbf{a}_1\,,\mathbf{a}^\dagger_2] = \mathbf{0} = [\,\mathbf{a}_2\,,\mathbf{a}^\dagger_1] \qquad (21.1.3)$$

All number-1 operators commute with all number-2 operators, but the operator commutation relations within the number-1 space or within the number-2 space remain the same as they were for a 1D-oscillator.

$$[\,\mathbf{a}_1, \mathbf{a}^\dagger_1] = \mathbf{1}\,,\quad [\,\mathbf{a}_2, \mathbf{a}^\dagger_2] = \mathbf{1} \qquad (21.1.4)$$

The commutation relations are summarized for all N-dimensional oscillator problems as follows.

$$[\,\mathbf{a}_m, \mathbf{a}_n] = \mathbf{a}_m\mathbf{a}_n - \mathbf{a}_n\mathbf{a}_m\,, \quad = \mathbf{0} \qquad (21.1.5a)$$

$$[\,\mathbf{a}_m, \mathbf{a}^\dagger_n] = \mathbf{a}_m\mathbf{a}^\dagger_n - \mathbf{a}^\dagger_n\mathbf{a}_m\,, \quad = \delta_{mn}\mathbf{1} \qquad (21.1.5b)$$

$$[\,\mathbf{a}^\dagger_m, \mathbf{a}^\dagger_n] = \mathbf{a}^\dagger_m\mathbf{a}^\dagger_n - \mathbf{a}^\dagger_n\mathbf{a}^\dagger_m\,, \quad = \mathbf{0}\,. \qquad (21.1.5c)$$

These are the **a**-operator equivalent of the orthonormality axiom-2 first given in Chapter 2.

Orthonormality and unit-scale relations (21.1.2) make it easy to find an **a**-operator expression for the 2D Hamiltonian (21.1.1).

$$\begin{aligned}\mathbf{H} = H_{11}\left(\mathbf{a}^\dagger_1\mathbf{a}_1 + \mathbf{1}/2\right) + \quad & H_{12}\mathbf{a}^\dagger_1\mathbf{a}_2 \qquad && = A\left(\mathbf{a}^\dagger_1\mathbf{a}_1 + \mathbf{1}/2\right) + (B - iC)\mathbf{a}^\dagger_1\mathbf{a}_2 \\ + H_{21}\mathbf{a}^\dagger_2\mathbf{a}_1 + H_{22}\left(\mathbf{a}^\dagger_2\mathbf{a}_2 + \mathbf{1}/2\right) & && + (B + iC)\mathbf{a}^\dagger_2\mathbf{a}_1 + D\left(\mathbf{a}^\dagger_2\mathbf{a}_2 + \mathbf{1}/2\right)\end{aligned} \qquad (21.1.6)$$

This expression was written on two lines in order to emphasize that the 2D quantum oscillator operator **H** has the form of the 2-state *ABCD* Hamiltonian **H** matrix (10.1.1b) used in Chapter 10.

$$\mathbf{H} = \begin{pmatrix} H_{11} & H_{12} \\ H_{21} & H_{22} \end{pmatrix} = \begin{pmatrix} A & B - iC \\ B + iC & D \end{pmatrix} \qquad (21.1.6b)$$

The ket-bras $|m\rangle\langle n|$ used in the latter are replaced by symmetrized $\mathbf{a}^\dagger_m\mathbf{a}_n$ operators. Both serve as elementary "place-holder" operators for the Hamiltonian components H_{mn} or parameters A, $B\pm iC$, and D.

$$|m\rangle\langle n| \to \left(\mathbf{a}^\dagger_m\mathbf{a}_n + \mathbf{a}_n\mathbf{a}^\dagger_m\right)/2 = \mathbf{a}^\dagger_m\mathbf{a}_n + \delta_{m,n}\mathbf{1}/2 \qquad (21.1.7)$$

The commutivity embodied in (21.1.5) is commonly known as *Bose symmetry* after Bose who first described the permutational symmetry of photons. The $(\mathbf{a}_m, \mathbf{a}^\dagger_n)$ operators are called *Boson operators* and the quanta or "particles" they create and destroy are known as *Bosons*.

Each time $\mathbf{a}^\dagger_m$ is used to raise quantum number of mode-m of an electromagnetic resonator (like the "Hall of Mirrors" cavity) it is equivalent to creating a new *photon*. If $\mathbf{a}^\dagger_m$ is used to raise the quantum number of mode-m of a molecule we can say we're creating a new *vibron*. Just put the suffix "-on" onto whatever your favorite oscillator motion is called and you have a cute name for your favorite Boson.

There exists an opposite kind of particle, the *Fermion* named after Enrico Fermi who is credited with describing the permutational anti-symmetry of electrons and nucleons. The creation-destruction operators for Fermions are defined in quite the opposite way using *anti-commutators* $\{\mathbf{A},\mathbf{B}\} = \mathbf{AB}+\mathbf{BA}$.

$$\{\mathbf{c}_m, \mathbf{c}_n\} = \mathbf{c}_m\mathbf{c}_n + \mathbf{c}_n\mathbf{c}_m \,, \quad = \mathbf{0} \qquad (21.1.8a)$$

$$\{\mathbf{c}_m, \mathbf{c}^\dagger_n\} = \mathbf{c}_m\mathbf{c}^\dagger_n + \mathbf{c}^\dagger_n\mathbf{c}_m \,, \quad = \delta_{mn}\mathbf{1} \qquad (21.1.8b)$$

$$\{\mathbf{c}^\dagger_m, \mathbf{c}^\dagger_n\} = \mathbf{c}^\dagger_m\mathbf{c}^\dagger_n + \mathbf{c}^\dagger_n\mathbf{c}^\dagger_m \,, \quad = \mathbf{0}\,. \qquad (21.1.8c)$$

The general two-dimensional Fermion Hamiltonian has ket-bras $|m\rangle\langle n|$ replaced by anti-symmetrized $\mathbf{c}^\dagger_m\mathbf{c}_n$ operators.

$$|m\rangle\langle n| \to \left(\mathbf{c}^\dagger_m\mathbf{c}_n - \mathbf{c}_n\mathbf{c}^\dagger_m\right)/2 = \mathbf{c}^\dagger_m\mathbf{c}_n - \delta_{m,n}\mathbf{1}/2 \qquad (21.1.7)$$

Fermi operators have a rigid birth-control policy; they are allowed only one Fermion or else, none at all. Creating two Fermions of the same type is punished by death. This is because $x=-x$ implies $x=0$.

$$\mathbf{c}^\dagger_m\mathbf{c}^\dagger_m|0\rangle = -\,\mathbf{c}^\dagger_m\mathbf{c}^\dagger_m|0\rangle = \mathbf{0} \qquad (21.1.8)$$

No two indistinguishable Fermions can occupy the same state. This is called the *Pauli exclusion principle*. Quantum numbers of $n=0$ and $n=1$ are the only allowed eigenvalues of the number operator.

$$\mathbf{c}^\dagger_m\mathbf{c}_m|0\rangle = \mathbf{0} \;,\; \mathbf{c}^\dagger_m\mathbf{c}_m|1\rangle = |1\rangle \;,\; \mathbf{c}^\dagger_m\mathbf{c}_m|n\rangle = \mathbf{0} \;\text{ for: } n>1 \qquad (21.1.9)$$

(b) Two-dimensional (or 2-particle) base states

A state for a particle moving in two-dimensions (or two one-dimensional particles) is described using *"ket-kets"* $|n_1\rangle|n_2\rangle$ which are outer products of the kets for each single dimension. The dual description is done similarly using *"bra-bras"* $\langle n_2|\langle n_1| = (|n_1\rangle|n_2\rangle)^\dagger$ which are outer products of the bras. This applies to all types of states $|\Psi_1\rangle|\Psi_2\rangle$ whether they are eigenstates $|n_1\rangle|n_2\rangle$, position states $|x_1\rangle|x_2\rangle$ and $\langle x_2|\langle x_1|$, coherent states $|\alpha_1\rangle|\alpha_2\rangle$ and $\langle\alpha_2|\langle\alpha_1|$, or whatever.

The scalar product is defined so that the two kinds of particles or dimensions will somehow "find" each other and completely ignore the presence of the other kind(s).

$$\langle x_2|\langle x_1|\Psi_1\rangle|\Psi_2\rangle = \langle x_1|\Psi_1\rangle\langle x_2|\Psi_2\rangle \qquad (21.1.10a)$$

This allows the probability axiom-1 to give the correct probability for, say, finding particle-1 at x_1 and particle-2 at x_2, if state $|\Psi_1\rangle|\Psi_2\rangle$ is forced to choose between all x_1 and x_2. Such a probability is a product

$$|\langle x_1, x_2|\Psi_1, \Psi_2\rangle|^2 = |\langle x_2|\langle x_1|\Psi_1\rangle|\Psi_2\rangle|^2 = |\langle x_1|\Psi_1\rangle|^2|\langle x_2|\Psi_2\rangle|^2 \qquad (21.1.10b)$$

of the individual probabilities $|\langle x_1|\Psi_1\rangle|^2$ and $\langle x_2|\Psi_2\rangle|^2$ according to standard probability theory. The shorthand big-bra-big-ket notation $\langle x_1, x_2|\Psi_1, \Psi_2\rangle$ for two-dimensional amplitudes $\langle x_2|\langle x_1|\Psi_1\rangle|\Psi_2\rangle$ is commonly used. Note the 1-2 ordering for both the big-bras and big-kets in the shorthand notation.

To gain a better understanding of the bra-bra and ket-ket structure we will ask the perennial modern question: "How would these structures be stored in a computer program?" The usual answer is in product arrays of some kind. Here we will sketch these objects.

We begin with an elementary ket basis for each dimension or particle type-1 and type-2.

$$\begin{matrix} Type-1 & & & & Type-2 & & & \cdots \end{matrix}$$

$$|0_1\rangle=\begin{pmatrix}1\\0\\0\\\vdots\end{pmatrix},\ |1_1\rangle=\begin{pmatrix}0\\1\\0\\\vdots\end{pmatrix},\ |2_1\rangle=\begin{pmatrix}0\\0\\1\\\vdots\end{pmatrix},\ \cdots \qquad |0_2\rangle=\begin{pmatrix}1\\0\\0\\\vdots\end{pmatrix},\ |1_2\rangle=\begin{pmatrix}0\\1\\0\\\vdots\end{pmatrix},\ |2_2\rangle=\begin{pmatrix}0\\0\\1\\\vdots\end{pmatrix},\ \cdots \quad (21.1.11a)$$

Then Cartesian or outer products are constructed for all states that might have non-zero amplitudes. And, therein lies a conflict between standard analysis and a finite computer. Each ket in (21.1.11) above is a column of ∞–dimensional and we are about to construct an ∞^2 number of things each of dimension ∞^2. A computer cannot handle a single ∞-dimensional ket let alone their outer products.

This is why the finite analysis of Sec. 7.3 is advocated. Constructing sets of adjustable finite sized model systems for each dimension systematizes state counting. Convergence is achieved by orderly upgrades in the number of model "pendulums." Outer products shown below are finite arrays indexed by oscillator quantum labels *0, 1, 2,...*(0-based indexing is the default mode in languages such as C^{++}.)

$$|0_1\rangle|0_2\rangle=\begin{pmatrix}1\\0\\0\\\vdots\end{pmatrix}\begin{pmatrix}1\\0\\0\\\vdots\end{pmatrix}=\begin{pmatrix}1\\0\\0\\\vdots\\\overline{0}\\0\\0\\0\\\vdots\\\overline{0}\\0\\0\\0\\\vdots\end{pmatrix},\ |0_1\rangle|1_2\rangle=\begin{pmatrix}1\\0\\0\\\vdots\end{pmatrix}\begin{pmatrix}0\\1\\0\\\vdots\end{pmatrix}=\begin{pmatrix}0\\1\\0\\\vdots\\\overline{0}\\0\\0\\0\\\vdots\\\overline{0}\\0\\0\\0\\\vdots\end{pmatrix},\ \cdots|1_1\rangle|0_2\rangle=\begin{pmatrix}0\\1\\0\\\vdots\end{pmatrix}\begin{pmatrix}1\\0\\0\\\vdots\end{pmatrix}=\begin{pmatrix}0\\0\\0\\\vdots\\\overline{1}\\0\\0\\0\\\vdots\\\overline{0}\\0\\0\\0\\\vdots\end{pmatrix},\ \cdots|1_1\rangle|2_2\rangle=\begin{pmatrix}0\\1\\0\\\vdots\end{pmatrix}\begin{pmatrix}0\\0\\1\\\vdots\end{pmatrix}=\begin{pmatrix}0\\0\\0\\\vdots\\\overline{0}\\0\\1\\\vdots\\\overline{0}\\0\\0\\0\\\vdots\end{pmatrix},\ (21.1.12a)$$

A 2-wave state product has a lexicographic *(00, 01, 02, ...10, 11, 12,..., 20, 21, 22, ..)* array indexing.

$$|\Psi_1\rangle|\Psi_2\rangle=\begin{pmatrix}\langle 0|\Psi_1\rangle\\\langle 1|\Psi_1\rangle\\\langle 2|\Psi_1\rangle\\\vdots\end{pmatrix}\otimes\begin{pmatrix}\langle 0|\Psi_2\rangle\\\langle 1|\Psi_2\rangle\\\langle 2|\Psi_2\rangle\\\vdots\end{pmatrix}=\begin{pmatrix}\langle 0|\Psi_1\rangle\langle 0|\Psi_2\rangle\\\langle 0|\Psi_1\rangle\langle 1|\Psi_2\rangle\\\langle 0|\Psi_1\rangle\langle 2|\Psi_2\rangle\\\vdots\\\overline{\langle 1|\Psi_1\rangle\langle 0|\Psi_2\rangle}\\\langle 1|\Psi_1\rangle\langle 1|\Psi_2\rangle\\\langle 1|\Psi_1\rangle\langle 2|\Psi_2\rangle\\\vdots\\\overline{\langle 2|\Psi_1\rangle\langle 0|\Psi_2\rangle}\\\langle 2|\Psi_1\rangle\langle 1|\Psi_2\rangle\\\langle 2|\Psi_1\rangle\langle 2|\Psi_2\rangle\\\vdots\end{pmatrix}=\begin{pmatrix}\langle 0_1 0_2|\Psi_1\Psi_2\rangle\\\langle 0_1 1_2|\Psi_1\Psi_2\rangle\\\langle 0_1 2_2|\Psi_1\Psi_2\rangle\\\vdots\\\overline{\langle 1_1 0_2|\Psi_1\Psi_2\rangle}\\\langle 1_1 1_2|\Psi_1\Psi_2\rangle\\\langle 1_1 2_2|\Psi_1\Psi_2\rangle\\\vdots\\\overline{\langle 2_1 0_2|\Psi_1\Psi_2\rangle}\\\langle 2_1 1_2|\Psi_1\Psi_2\rangle\\\langle 2_1 2_2|\Psi_1\Psi_2\rangle\\\vdots\end{pmatrix} \quad (21.1.12b)$$

The same indexing is used for the general 2-particle or 2-dimensional state $|\Psi\rangle$.

$$|\Psi\rangle = \begin{pmatrix} \langle 0_1 0_2|\Psi\rangle \\ \langle 0_1 1_2|\Psi\rangle \\ \langle 0_1 2_2|\Psi\rangle \\ \vdots \\ \hline \langle 1_1 0_2|\Psi\rangle \\ \langle 1_1 1_2|\Psi\rangle \\ \langle 1_1 2_2|\Psi\rangle \\ \vdots \\ \hline \langle 2_1 0_2|\Psi\rangle \\ \langle 2_1 1_2|\Psi\rangle \\ \langle 2_1 2_2|\Psi\rangle \\ \vdots \end{pmatrix} = \begin{pmatrix} \Psi_{00} \\ \Psi_{01} \\ \Psi_{02} \\ \vdots \\ \hline \Psi_{10} \\ \Psi_{11} \\ \Psi_{12} \\ \vdots \\ \hline \Psi_{20} \\ \Psi_{21} \\ \Psi_{22} \\ \vdots \end{pmatrix} \qquad (21.1.12c)$$

A word of caution: Do *NOT* assume that a general two-particle state $|\Psi\rangle$ can be written as a single outer product $|\Psi_1\rangle|\Psi_2\rangle$ (or even rarer, as $|\Psi_1\rangle|\Psi_1\rangle$) of two single-particle states $|\Psi_1\rangle$ and $|\Psi_2\rangle$. This would be as unusual as having a general matrix operator **M** be a single nilpotent operator $|1\rangle\langle 2|$ or idempotent $|1\rangle\langle 1|$, both of which are singular, that is, have zero determinant. Rather, a general matrix **M** is a full combination

$$\mathbf{M} = \sum_m \sum_n M_{m,n} |m\rangle\langle n|$$

of all possible ket-bra elementary operator products $|m\rangle\langle n|$. So, also, is a general state like (21.1.11) a combination of all possible ket-ket products $|x_1\rangle|x_2\rangle$ made from whichever basis is currently being used.

$$|\Psi\rangle = \sum_m \sum_n \Psi_{m,n} |m\rangle|n\rangle \qquad (21.1.12d)$$

(c) Two-dimensional (or 2-particle) matrix operators

When a two-dimensional operator acts on a two-dimensional state, each dimension or particle type-1 or type-2 operator "finds" its corresponding type in the state and goes to work on it while ignoring the other type(s). For creation and destruction operations defined in (20.2.13b) the following happens.

$$\mathbf{a}_1^\dagger |n_1 n_2\rangle = \mathbf{a}_1^\dagger |n_1\rangle|n_2\rangle = \sqrt{n_1+1}\,|n_1+1\, n_2\rangle \quad , \qquad \mathbf{a}_2^\dagger |n_1 n_2\rangle = |n_1\rangle \mathbf{a}_2^\dagger |n_2\rangle = \sqrt{n_2+1}\,|n_1\, n_2+1\rangle$$

$$\mathbf{a}_1 |n_1 n_2\rangle = \mathbf{a}_1 |n_1\rangle|n_2\rangle = \sqrt{n_1}\,|n_1-1\, n_2\rangle \quad , \qquad \mathbf{a}_2 |n_1 n_2\rangle = |n_1\rangle \mathbf{a}_2 |n_2\rangle = \sqrt{n_2}\,|n_1\, n_2-1\rangle$$

(21.1.13a) (21.1.13b)

This is consistent with the following general definition of the 2D oscillator base state.

$$|n_1 n_2\rangle = \frac{\left(\mathbf{a}_1^\dagger\right)^{n_1}\left(\mathbf{a}_2^\dagger\right)^{n_2}}{\sqrt{n_1!\, n_2!}}|0\,0\rangle \qquad (21.1.14)$$

The $\mathbf{a}_m^\dagger \mathbf{a}_n$ combinations in the *ABCD* Hamiltonian **H** in (21.1.6) have fairly simple matrix elements.

$$\mathbf{a}_1^\dagger \mathbf{a}_1 |n_1 n_2\rangle = n_1 |n_1\, n_2\rangle \quad , \qquad \mathbf{a}_1^\dagger \mathbf{a}_2 |n_1 n_2\rangle = \sqrt{n_1+1}\sqrt{n_2}\,|n_1+1\, n_2-1\rangle$$

$$\mathbf{a}_2^\dagger \mathbf{a}_1 |n_1 n_2\rangle = \sqrt{n_1}\sqrt{n_2+1}\,|n_1-1\, n_2+1\rangle \quad , \qquad \mathbf{a}_2^\dagger \mathbf{a}_2 |n_1 n_2\rangle = n_2 |n_1\, n_2\rangle \qquad (21.1.15a)$$

Part of the matrix representation of **H** in creation basis (21.1.14) is shown below.

$\langle \mathbf{H} \rangle = A(\mathbf{1}/2) + D(\mathbf{1}/2) +$

	$\|00\rangle$	$\|01\rangle$	$\|02\rangle$	$\cdots$	$\|10\rangle$	$\|11\rangle$	$\|12\rangle$	$\cdots$	$\|20\rangle$	$\|21\rangle$	$\|22\rangle$	$\cdots$
$\langle 00\|$	0			$\cdots$	$\cdot$			$\cdots$				$\cdots$
$\langle 01\|$		D		$\cdots$	$B+iC$	$\cdot$		$\cdots$				$\cdots$
$\langle 02\|$			$2D$	$\cdots$		$\sqrt{2}(B+iC)$	$\cdot$	$\cdots$				$\cdots$
$\vdots$	$\vdots$	$\vdots$	$\vdots$	$\ddots$	$\vdots$	$\vdots$	$\vdots$	$\ddots$				$\cdots$
$\langle 10\|$	$\cdot$	$B-iC$		$\cdots$	A			$\cdots$	$\cdot$			$\cdots$
$\langle 11\|$		$\cdot$	$\sqrt{2}(B-iC)$	$\cdots$		$A+D$		$\cdots$	$\sqrt{2}(B+iC)$	$\cdot$		$\cdots$
$\langle 12\|$			$\cdot$	$\cdots$			$A+2D$	$\cdots$		$\sqrt{4}(B+iC)$	$\cdot$	$\cdots$
$\vdots$	$\vdots$	$\vdots$	$\vdots$	$\ddots$	$\vdots$	$\vdots$	$\vdots$	$\ddots$	$\vdots$	$\vdots$	$\vdots$	$\ddots$
$\langle 20\|$					$\cdot$	$\sqrt{2}(B-iC)$		$\cdots$	$2A$			$\cdots$
$\langle 21\|$						$\cdot$	$\sqrt{4}(B-iC)$	$\cdots$		$2A+D$		$\cdots$
$\langle 22\|$							$\cdot$	$\cdots$			$2A+2D$	$\cdots$
$\vdots$					$\vdots$	$\vdots$	$\vdots$	$\ddots$	$\vdots$	$\vdots$	$\vdots$	$\ddots$

(21.1.15b)

The eigenstates and eigenvalues for this monster matrix will solve the general quantum 2D harmonic oscillator problem. A little rearrangement of rows and columns brings the matrix to a block-diagonal form in which base states $|n_1\rangle|n_2\rangle$ with the same *total quantum number* $\nu = n_1 + n_2$ are adjacent.

$\langle \mathbf{H} \rangle = A(\mathbf{1}/2) + D(\mathbf{1}/2) +$

	$\|00\rangle$	$\|01\rangle$	$\|10\rangle$	$\|02\rangle$	$\|11\rangle$	$\|20\rangle$	$\|03\rangle$	$\|12\rangle$	$\|21\rangle$	$\|30\rangle$	$\cdots$
$\langle 00\|$	0										
$\langle 01\|$		D	$B+iC$								
$\langle 10\|$		$B-iC$	A								
$\langle 02\|$				$2D$	$\sqrt{2}(B+iC)$						
$\langle 11\|$				$\sqrt{2}(B-iC)$	$A+D$	$\sqrt{2}(B+iC)$					
$\langle 20\|$					$\sqrt{2}(B-iC)$	$2A$					
$\langle 03\|$							$3D$	$\sqrt{3}(B+iC)$			
$\langle 12\|$							$\sqrt{3}(B-iC)$	$A+2D$	$\sqrt{4}(B+iC)$		
$\langle 21\|$								$\sqrt{4}(B-iC)$	$2A+D$	$\sqrt{3}(B+iC)$	
$\langle 30\|$									$\sqrt{3}(B-iC)$	$3A$	
$\vdots$											

(21.1.15c)

Note the 2-by-2 sub-space $|n_1 n_2\rangle = \{|01\rangle, |10\rangle\}$ with total quantum number $\nu = 1$. It supports a matrix that is identical to the original 2-by-2 Hamiltonian (21.1.6b). (Except, it is up side down and has the zero-point unit matrix added.) A sub-space with unit total quantum number is called the *fundamental* ($\nu = 1$) vibrational sub-space. Similarity of classical and ($\nu = 1$) quantum matrices means the fundamental quantum eigenvectors are the same as the classical A, B, AB or C normal mode vectors discussed in Sec. 10.2(a, b, c) and Sec. 10.3(a-b). This leads to analytical solutions to all quantum matrices (21.1.15c).

(d) 2D-Oscillator eigensolutions

The analogy between classical 2D-oscillators and a 2-state quantum systems was developed in Sec. 10.5 and solved by special unitary (*SU(2)*) or rotation (*R(3)*) group algebra in Appendices 10.A-B. These solutions lead to solutions for the quantum 2D-oscillator Hamiltonian given above in (21.1.15c-d).

(1) Fundamental eigenstates

The first step is to diagonalize the fundamental 2-by-2 matrix given in (21.1.15c-d).

$$\langle \mathbf{H} \rangle_{\upsilon=1}^{Fundamental} = \begin{array}{c|cc} n_1,n_2 & |1,0\rangle & |0,1\rangle \\ \hline \langle 1,0| & A & B-iC \\ \langle 0,1| & B+iC & D \end{array} + \frac{A+D}{2}\mathbf{1} \qquad (21.1.16)$$

Here we have turned the matrix right-side-up so it matches the Hamiltonian solved in (10.5.10). (A choice of "Little-Endian" indexing (... *10, 01, ...20,11,21...*) instead of "Big-Endian" indexing (...*01,10, ...02,1...*) reorders the states to match.) The eigensolution (10.5.10) uses the Hamilton decomposition coefficients to define a rotation-crank angular rate vector $\boldsymbol{\Omega}$

$$\boldsymbol{\Omega} = (\Omega_X, \Omega_Y, \Omega_Z) = (2B, 2C, A\text{-}D) = (\Omega_B, \Omega_C, \Omega_A)\,, \qquad (21.1.17)$$

and the average overall phase rate (including zero-point term $(A+D)/2$) is

$$\Omega_0 = A+D. \qquad (21.1.18)$$

This gives **H** as follows

$$\begin{pmatrix} A & B-iC \\ B+iC & D \end{pmatrix} + \frac{A+D}{2}\mathbf{1} = (A+D)\begin{pmatrix} 1 & 0 \\ 0 & 1 \end{pmatrix} + 2B\begin{pmatrix} 0 & 1 \\ 1 & 0 \end{pmatrix}\frac{1}{2} + 2C\begin{pmatrix} 0 & -i \\ i & 0 \end{pmatrix}\frac{1}{2} + (A-D)\begin{pmatrix} 1 & 0 \\ 0 & -1 \end{pmatrix}\frac{1}{2}$$

in terms of Jordan-Pauli spin operators. (21.1.19)

$$\mathbf{H} = \Omega_0\mathbf{1} + \boldsymbol{\Omega}\bullet\vec{\mathbf{S}} = \Omega_0\mathbf{1} + \Omega_B\mathbf{S}_B + \Omega_C\mathbf{S}_C + \Omega_A\mathbf{S}_A \quad (ABC\ \textit{Optical vector notation})$$
$$= \Omega_0\mathbf{1} + \Omega_X\mathbf{S}_X + \Omega_Y\mathbf{S}_Y + \Omega_Z\mathbf{S}_Z \quad (XYZ\ \textit{Electron spin notation})$$

The frequency eigenvalues $\omega_\pm$ of $\mathbf{H}\text{-}\Omega_0\mathbf{1}/2$ and *fundamental transition frequency* $\Omega = \omega_+ - \omega_-$ are

$$\omega_\pm = \frac{\Omega_0 \pm \Omega}{2} = \frac{A+D \pm \sqrt{(2B)^2+(2C)^2+(A-D)^2}}{2}$$
$$= \frac{A+D}{2} \pm \sqrt{\left(\frac{A-D}{2}\right)^2 + B^2 + C^2} \qquad (21.1.20a)$$

$\boldsymbol{\Omega}$ "points out" eigenvectors whose spin vectors **S** align or anti-align with the $\boldsymbol{\Omega}$-vector of **H**. The polar angles of the **S**-vector are Euler angles (α,β) in Fig. 10.5.8. Equating (α,β) in an Euler state (10.A.1a) to polar angles (φ,ϑ) of the $+\boldsymbol{\Omega}$-vector (or polar angles $(\varphi,\vartheta\pm\pi)$ of the $-\boldsymbol{\Omega}$-vector) gives **H** eigenvectors.

$$|\omega_+\rangle = \begin{pmatrix} e^{-i\varphi/2}\cos\frac{\vartheta}{2} \\ e^{i\varphi/2}\sin\frac{\vartheta}{2} \end{pmatrix}, \quad |\omega_-\rangle = \begin{pmatrix} -e^{-i\varphi/2}\sin\frac{\vartheta}{2} \\ e^{i\varphi/2}\cos\frac{\vartheta}{2} \end{pmatrix} \quad \text{where:} \begin{cases} \cos\vartheta = \frac{A\text{-}D}{\Omega} \\ \tan\varphi = \frac{C}{B} \end{cases} \qquad (21.1.20b)$$

The ket eigenvectors are being expressed in terms of $\{|10\rangle, |01\rangle\}$ bases.

$$|\omega_+\rangle = e^{-i\varphi/2}\left(\cos\frac{\vartheta}{2}|10\rangle + e^{i\varphi}\sin\frac{\vartheta}{2}|01\rangle\right), \quad |\omega_-\rangle = e^{-i\varphi/2}\left(-\sin\frac{\vartheta}{2}|10\rangle + e^{i\varphi}\cos\frac{\vartheta}{2}|01\rangle\right) \quad (21.1.20c)$$

More important for the general solution, are the *eigen-creation operators* $\mathbf{a}^\dagger_+$ *and* $\mathbf{a}^\dagger_-$ defined by

$$\mathbf{a}^\dagger_+ = e^{-i\varphi/2}\left(\cos\frac{\vartheta}{2}\mathbf{a}^\dagger_1 + e^{i\varphi}\sin\frac{\vartheta}{2}\mathbf{a}^\dagger_2\right), \quad \mathbf{a}^\dagger_- = e^{-i\varphi/2}\left(-\sin\frac{\vartheta}{2}\mathbf{a}^\dagger_1 + e^{i\varphi}\cos\frac{\vartheta}{2}\mathbf{a}^\dagger_2\right) \quad (21.1.20d)$$

The $\mathbf{a}^\dagger_\pm$ create **H** eigenstates (21.1.20c) directly from the ground state.

$$\mathbf{a}^\dagger_+|0\rangle = |\omega_+\rangle, \quad \mathbf{a}^\dagger_-|0\rangle = |\omega_-\rangle \quad (21.1.20e)$$

In terms of the eigen-$\mathbf{a}^\dagger_\pm$ operators, the Hamiltonian has zero off-diagonal components *(B=0=C)* and is reduced to (at worst) an *A*-type (Asymmetric Diagonal) or $C_2{}^A$-symmetric operator described in Sec. 10.2(a). But, if the eigenvalues are degenerate ($\omega_+ = \omega_-$) then **H** is a fully *SU(2)* symmetric unit 2-by-2 Hamiltonian like the case where *(B=0=C)* and *(A=D)*.

Setting *(B=0=C)* and *(A=*ω_+*)* and *(D=*ω_-*)* in (21.1.15c) gives diagonal block matrices.

$$\langle \mathbf{H} \rangle = A(\mathbf{1}/2) + D(\mathbf{1}/2) +$$

	$\|00\rangle$	$\|01\rangle$ $\|10\rangle$	$\|02\rangle$ $\|11\rangle$ $\|20\rangle$	$\|03\rangle$ $\|12\rangle$ $\|21\rangle$ $\|30\rangle$	⋯
$\langle 00\|$	0				
$\langle 01\|$		ω_-			
$\langle 10\|$		ω_+			
$\langle 02\|$			$2\omega_-$		
$\langle 11\|$			$\omega_+ + \omega_-$		
$\langle 20\|$			$2\omega_+$		
$\langle 03\|$				$3\omega_-$	
$\langle 12\|$				$\omega_+ + 2\omega_-$	
$\langle 21\|$				$2\omega_+ + \omega_-$	
$\langle 30\|$				$3\omega_+$	
⋮					

(21.1.21)

The eigenvalue splitting pattern shown in Fig. 21.1.1 is a function of the fundamental splitting frequency.

$$\omega_+ - \omega_- = \Omega = \sqrt{(2B)^2 + (2C)^2 + (A-D)^2} = A - D \quad (21.1.22)$$

For *SU(2)* symmetry ($\Omega=0$) the spectrum reduces to perfect harmonically spaced levels of eigen-frequency $\omega=\upsilon+1$ and degeneracy $\upsilon+1 = 1, 2, 3, 4$, ...for each total quantum number $\upsilon = 0, 1, 2, 3, ...$, respectively. As will be shown later, this is precisely analogous to the spin angular momentum quantum *multiplet* levels of total angular momentum quantum numbers $j = 0, 1/2, 1, 3/2, ...$ In fact, each degenerate level corresponds to a different irep of *SU(2)* and the integral $j = 0,1, 2,...$ correspond to ireps of the related rotation group *R(3)* in three dimensions. What we have here is a very powerful way to understand and derive the quantum theory of angular momentum.

As the splitting frequency increases each multiplet splits entirely since the symmetry is reduced to a commutative $C_2{}^{A,B,or C}$ subgroup of *SU(2)* that does not require degeneracy. Every level differs from the nearest neighbor in its multiplet by the same transition frequency Ω. So no matter what the value of the

parameters {*A*, *B*, *C*, *D*}, this model maintains its harmonic spectrum to some extent. However, at rational values of the ratio Ω/ω, there will occur a varying number of degeneracies between levels split off from different multiplets and some interesting effects in the classical and quantum dynamics.

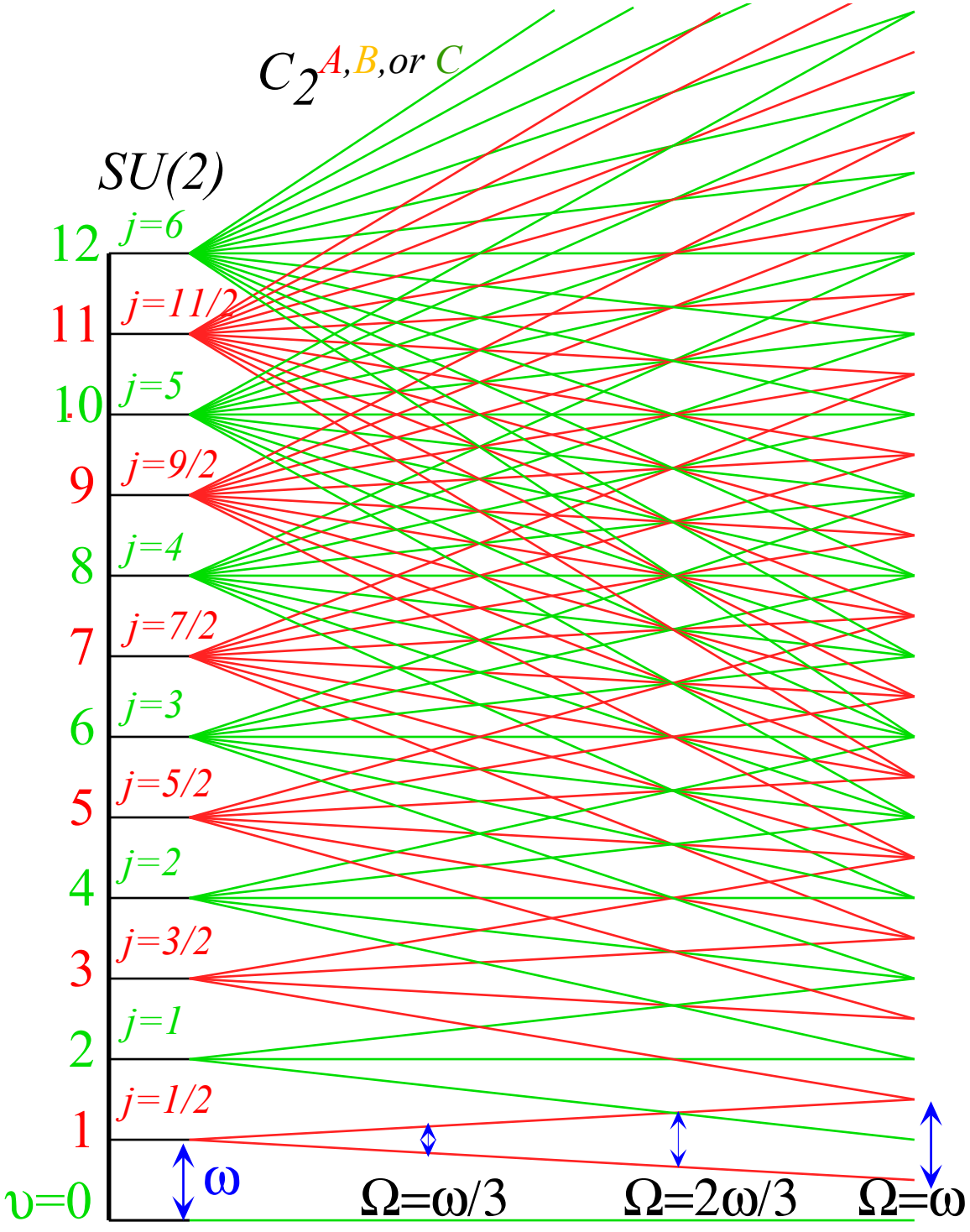

Fig. 21.1.1 Two-Dimensional harmonic oscillator levels with SU(2) degeneracy and C_2 splitting.

(2) U(2)⊃C_2^A eigenstates and wavefunctions

The simplest examples of 2D oscillator eigensolutions are found for the type-*A* or *Asymmetric Diagonal* Hamiltonian **H** in (21.1.1) for which only the parameters *A* and *D* are non-zero. *(B=0=C)*

$$\mathbf{H}^A = \frac{A}{2}\left(\mathbf{p}_1^2 + \mathbf{x}_1^2\right) + \frac{D}{2}\left(\mathbf{p}_2^2 + \mathbf{x}_2^2\right) \qquad (21.1.23)$$

In terms of **a**-operators, **H** in (21.1.6) reduces to sums of number operators $\mathbf{a}^\dagger_m\,\mathbf{a}_m$ or unit operator **1**.

$$\mathbf{H}^A = A\left(\mathbf{a}_1^\dagger\mathbf{a}_1 + \mathbf{1}/2\right) + D\left(\mathbf{a}_2^\dagger\mathbf{a}_2 + \mathbf{1}/2\right) \qquad (21.1.24)$$

Then the **H** matrix (21.1.15) is diagonal, and the eigenvalues are simple combinations of quanta n_1 and n_2.

$$\begin{aligned}\varepsilon^A_{n_1n_2} &= A\left(n_1 + \frac{1}{2}\right) + D\left(n_2 + \frac{1}{2}\right) = \frac{A+D}{2}(n_1+n_2+1) + \frac{A-D}{2}(n_1-n_2) \\ &= \Omega_0(n_1+n_2+1) + \frac{\Omega}{2}(n_1-n_2) = \Omega_0(\upsilon+1) + \Omega\, m\end{aligned} \qquad (21.1.25a)$$

Here *total quantum number* υ and half-difference or *asymmetry quantum number m*

$$\upsilon = n_1 + n_2 \quad , \qquad m = \frac{n_1 - n_2}{2} \qquad (21.1.25b)$$

multiply the *fundamental frequency* $\Omega_0=\omega$ and *splitting 1/2-beat frequency* Ω as seen in Fig. 21.1.2.

$$\omega = \Omega_0 = \frac{A+D}{2} \quad , \quad \Omega = \frac{A-D}{2} \qquad (21.1.25c)$$

The eigenstates for the asymmetric-diagonal $\mathbf{H}^A$ Hamiltonian are just the base states from (21.1.14).

$$|n_1n_2\rangle = \frac{\left(\mathbf{a}_1^\dagger\right)^{n_1}\left(\mathbf{a}_2^\dagger\right)^{n_2}}{\sqrt{n_1!\,n_2!}}|0\,0\rangle \qquad (21.1.26)$$

The eigenstates belong to the symmetry $C_2{}^A$ first discussed in Sec. 10.2(a) and listed near the left hand side of Fig. 10.4.2. The two x_1 and x_2 fundamental normal mode classical vibrations associated with this symmetry are shown in Fig. 10.2.1. If these two motions have the same frequency *(A=D)* then the symmetry is much higher, indeed. The *(A=D)*-case has the full *U(2) symmetry* that a 2D oscillator can have as indicated on the extreme left hand side of Fig. 10.4.2. The *U(2)*-symmetric Hamiltonian

$$\mathbf{H}^{U(2)} = E\left(\mathbf{a}_1^\dagger\mathbf{a}_1 + \mathbf{a}_2^\dagger\mathbf{a}_2 + \mathbf{1}\right) \quad where: \quad A = E = D \qquad (21.1.27a)$$

has the same eigenvalues as a 1D harmonic oscillator with the zero-point increased from 1/2 to 1.

$$\varepsilon^{U(2)}_{n_1n_2} = \Omega_0(n_1+n_2+1) = \omega(\upsilon+1) \quad (u = 0,1,2,3...) \qquad (21.1.27b)$$

However, the degeneracy of the υ-th level is equal to the total quantum number υ as was shown in Fig. 21.1.2 on the extreme left hand side where the splitting frequency Ω is zero.

The redux of the 1D spectrum in a $C_2{}^A$-symmetric two-dimensional system is not surprising if you consider the two-pendulum analogy in Fig. 10.1.1 with equal pendulums or in Fig. 10.2.3 with the coupling spring removed. The result is two independent pendulums. The only effect of having two of them is that the energy level degeneracy and zero-point goes up, but they're just 1D levels.

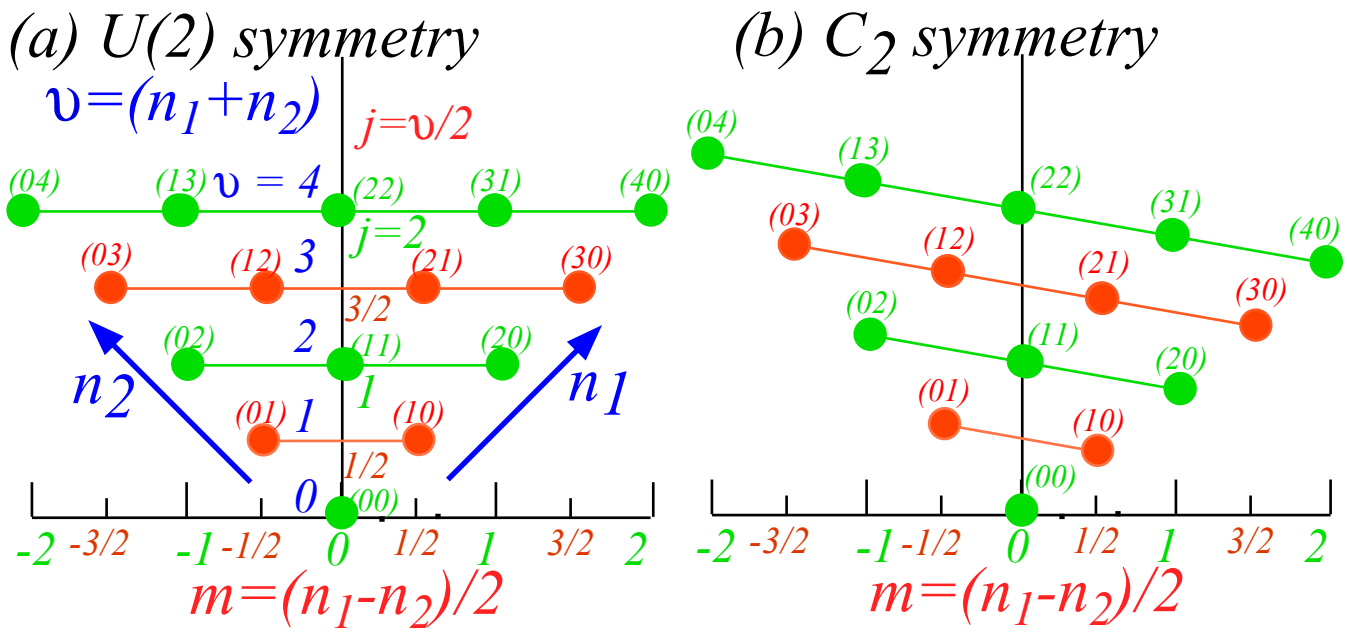

Fig. 21.1.2 Two-Dimensional harmonic oscillator quanta with (a)U(2) degeneracy and (b) C_2 splitting.

A sketch of the energy-quantum-number relation (21.1.27) is shown in Fig. 21.1.2. With U*(2)* symmetry (Ω=0), the degenerate energy values lie along a horizontal line. The states $|(n_1,n_2)\rangle$ with larger n_1 appear proportionally farther to the right while those with larger n_2 sit to the left. As Ω becomes non-zero the lines tip in proportion to Ω and the reduction of *U(2)* to a C_2 symmetry shows up in the splitting of the degenerate levels. The splitting seen in Fig. 21.1.1 is a vertical projection of the tipped points in Fig. 21.1.2 with the n_1 vibrations assumed to be slower *(A<D)* so they lose frequency in proportion to n_1 while the faster n_2 states gain in proportion to their quantum n_2 -values.

(3) U(2)⊃C_2^A oscillator wavefunctions

A two-dimensional oscillator eigenfunction is a simple product of two one-dimensional functions.

$$\langle x_1 x_2|n_1 n_2\rangle = \langle x_1|n_1\rangle\langle x_2|n_2\rangle$$

For example, the ground state eigenfunction $\langle x_1 x_2|0\,0\rangle$ follows from (20.2.7c) with scale $M\omega/\hbar=1$.

$$\psi_{00}(x_1,x_2) = \langle x_1|0\rangle\langle x_2|0\rangle = \frac{e^{-x_1^2/2}}{(\pi)^{1/4}}\frac{e^{-x_2^2/2}}{(\pi)^{1/4}} = \frac{e^{-\left(x_1^2+x_2^2\right)/2}}{(\pi)^{1/2}} \qquad (21.1.28)$$

This (υ=0) Gaussian is plotted in Fig. 21.1.3, and the (υ=1) excited state wave doublet in Fig. 21.1.3.

$$\psi_{10}(x_1,x_2) = \frac{\sqrt{2}x_1 e^{-\left(x_1^2+x_2^2\right)/2}}{(\pi)^{1/2}}\ , \quad \psi_{01}(x_1,x_2) = \frac{\sqrt{2}x_2 e^{-\left(x_1^2+x_2^2\right)/2}}{(\pi)^{1/2}} \qquad (21.1.29)$$

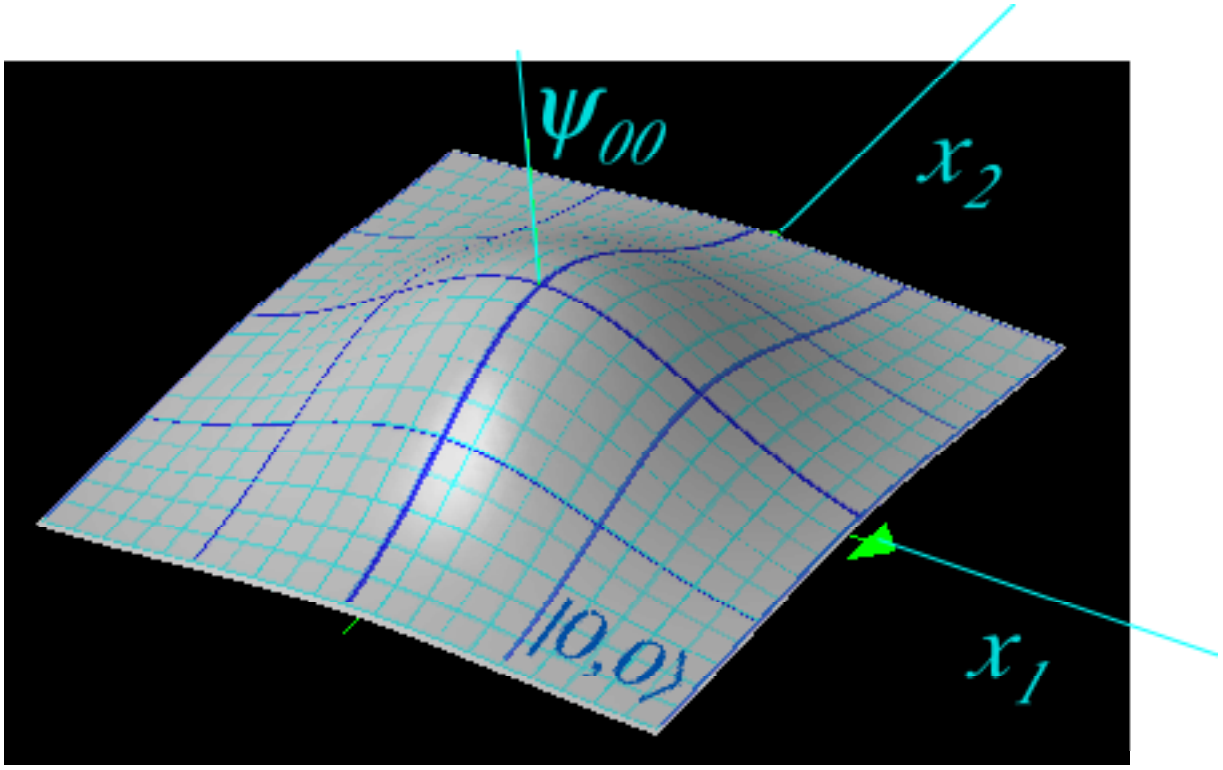

Fig. 21.1.3 2-D harmonic oscillator ground state wave function $\Psi_{00}(x_1,x_2)$

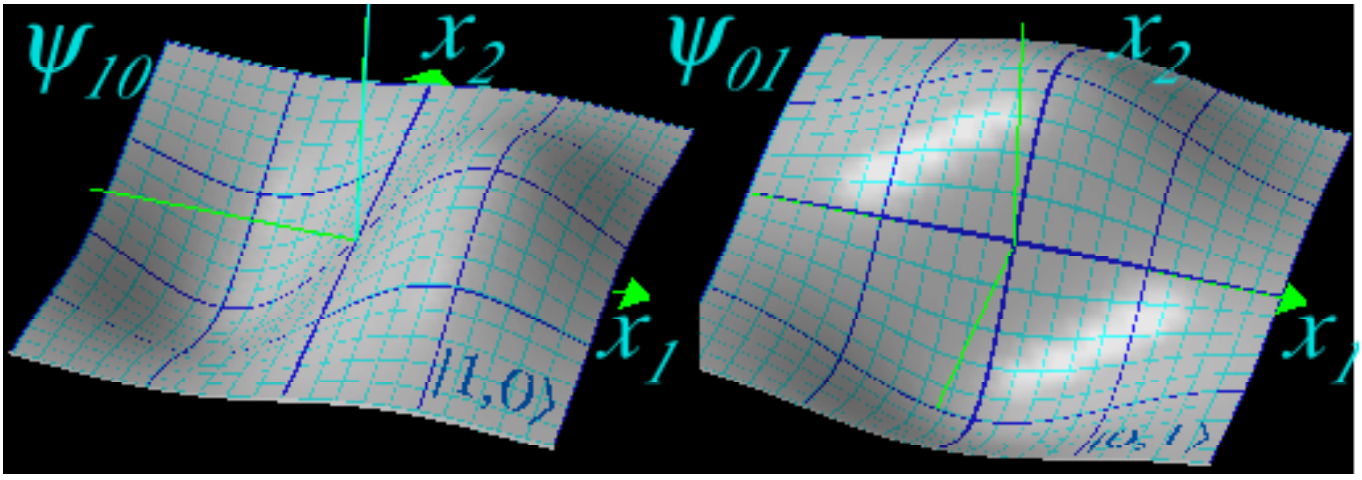

Fig. 21.1.4 2-D harmonic oscillator first excited state wave functions: $\Psi_{10}(x_1,x_2)$ *and* $\Psi_{01}(x_1,x_2)$.

The two components of the doublet are related by a 90° rotation in the (x_1,x_2)-plane. Here, we are looking at the real part of waves that each have their usual complex time factor $e^{-i\varepsilon_n t/\hbar}$ which in this case is a different frequency $\omega_{n_1 n_2} = e_{n_1 n_2}/\hbar$ given by (21.1.25a) for each, in general. So these pictures represent snapshots of standing waves that oscillate up and down just like their 1D ancestors in Fig. 20.2.1.

However, their probability distributions shown below in Fig. 21.1.5 are motionless as must be any distribution for a pure-energy eigenstate. The squared wavefunctions are greater than zero everywhere and falls off more rapidly for large x.

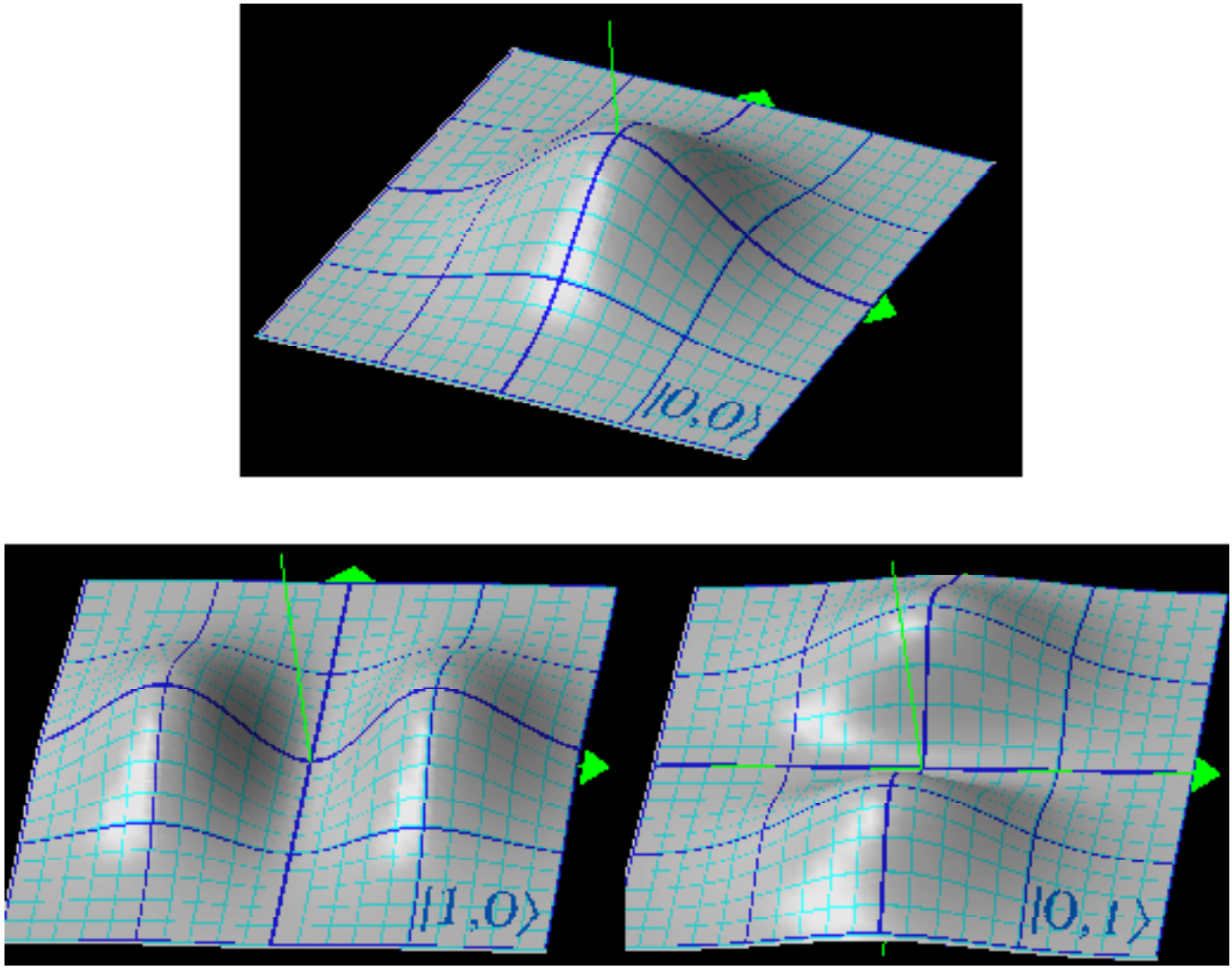

Fig. 21.1.5 2-D oscillator probability distributions: $|\Psi_{00}(x_1,x_2)|^2$, $|\Psi_{10}(x_1,x_2)|^2$, *and* $|\Psi_{01}(x_1,x_2)|^2$.

Combination wave functions, on the other hand, have moving probability distributions if their component states have different eigenfrequencies. Consider for example, the 50-50 combination of the first two excited states $|1\,0\rangle$ and $|0\,1\rangle$ whose probability distributions are shown for three different times in Fig. 21.1.6. The result is the quantum version of the classical beats shown in Fig. 10.2.2 for uncoupled oscillators and in Fig. 10.2.5 and Fig. 10.2.6 for coupled bilaterally symmetric oscillators.

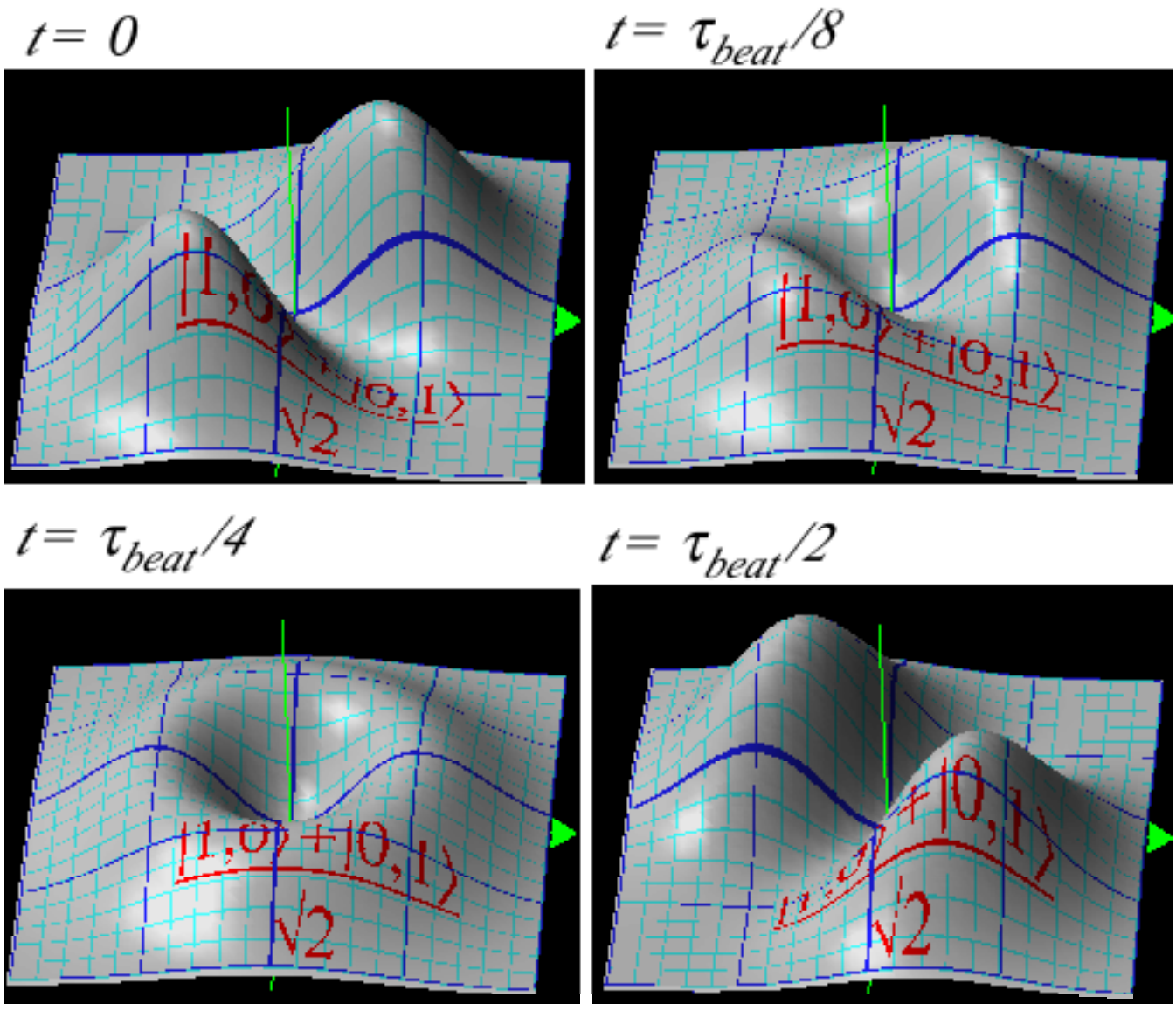

Fig. 21.1.6 2-D oscillator probability distributions: $|\, e^{-i\omega_{10}\, t/\hbar}\, \Psi_{10}(x_1,x_2) + e^{-i\omega_{01}\, t/\hbar}\, \Psi_{01}(x_1,x_2)|^2$.

The time-dependent wavefunction plotted in Fig. 21.1.6 oscillates with beat period $\tau_{beat} = 2\pi/\,(\omega_{10}-\omega_{01})$.

$$\Psi(x_1,x_2,t) = \frac{1}{2}\left|\psi_{10}(x_1,x_2)\,e^{-i\omega_{10}t} + \psi_{01}(x_1,x_2)\,e^{-i\omega_{01}t}\right|^2 e^{-\left(x_1^2+x_2^2\right)} = \frac{e^{-\left(x_1^2+x_2^2\right)}}{2\pi}\left|\sqrt{2}x_1 e^{-i\omega_{10}t} + \sqrt{2}x_1 e^{-i\omega_{01}t}\right|^2$$

$$= \frac{e^{-\left(x_1^2+x_2^2\right)}}{\pi}\left(x_1^2+x_2^2+2x_1x_2\cos\left(\omega_{10}-\omega_{01}\right)t\right) = \frac{e^{-\left(x_1^2+x_2^2\right)}}{\pi}\begin{cases}\left|x_1+x_2\right|^2 & for:\ t=0\\ x_1^2+x_2^2 & for:\ t=\tau_{\text{beat}}/4\\ \left|x_1-x_2\right|^2 & for:\ t=\tau_{\text{beat}}/2\end{cases} \qquad (21.1.30)$$

At one quarter of beat period (τ_{beat} /4) a circular distribution appears. It is equivalent to the 1/4-wave circular polarization motion shown in the classical model by Fig. 10.2.6(a). The pictures above will apply exactly to a *B*-type oscillator if they are all rotated by *45°* in the *(x_1x_2)*-plane.

21.2 2D Oscillator Symmetry, Spin, and Wavefunctions

For a given cranking frequency Ω, the eigenvalues shown in Fig. 21.1.1 are the same no matter what values we choose for the parameters *{A, B, C, D}*. However, the eigenvectors or states depend acutely on parameter values as do the underlying symmetries and physics.

The Abelian symmetry analysis in Chapter 8-9 uses C_6 symmetry to dictate a fixed set of eigenvectors, but their eigenvalues depend on the values of six **H**-parameters. However, for non-Abelian D_3 or D_6 symmetry analysis in Chapter 15, both eigenvalues and eigenvectors may vary with the **H**-parameters and the eigenstates may have a range of different local symmetry subgroups and correspondingly different physics. Different choices for local symmetry subgroups or *Maximal Sets of Commuting Observables (MSOCO)* such as in Fig. 15.2.1, gives different types of symmetry states and wave dynamics. So it is with *U(2)* symmetry that is an infinite non-Abelian group. Its subgroups correspond to a range of different eigensolutions.

For the *U(2)* model, all parameters *{A, B, C, D}* have basically the same eigenvalues for a given Ω as shown in Fig. 21.1.1, but the eigenvectors or eigenstates will vary according to which *U(2)* subgroups C_2^A*(Asymmetric diagonal)*, C_2^B*(Bilateral)*, C_2^{AB}*(Mixed AB)*, C_2^C*(Circular)*, or C_1^{ABCD}*(Elliptical)* listed in the *U(2)* catalog of Fig. 10.4.2 are the Abelian sub-group symmetries of the **H**-Hamiltonian. The classical two-dimensional-oscillator and analogous quantum two-state eigenstates for these symmetries are compared in Sections 10.2(a), 10.2(b), 10.3(a-b), 10.2(c), and 10.4(a-b), respectively. Now we compare the corresponding quantum two-dimensional-oscillators having these symmetries. Of these, C_2^C *(Circular)* is most useful for understanding quantum angular momentum.

(a) Angular momentum eigenstates: C_2^C symmetry

Consider having the *C*-parameter be non-zero.*(A=D, B=0, C≠0.)* According to Sec. 2.9(c) this corresponds to physics with "*C-ness*", that is, chirality, circular polarization, current states, Coriolis splitting, cyclotron resonance, and anything resembling moving waves with definite right or left-handed momenta. From (21.1.1) with *A=D, B=0, C≠0,* we have

$$\mathbf{H}^C = \frac{A}{2}\left(\mathbf{p}_1^2+\mathbf{x}_1^2+\mathbf{p}_2^2+\mathbf{x}_2^2\right)+C\left(\mathbf{x}_1\mathbf{p}_2-\mathbf{x}_2\mathbf{p}_1\right) \qquad (21.2.1a)$$

Note that $\mathbf{H}^C$ contains a term that is *C*-times the two-dimensional *angular momentum operator* $\mathbf{l}_3$.

$$\mathbf{l}_3 = \mathbf{x}_1\mathbf{p}_2-\mathbf{x}_2\mathbf{p}_1 \qquad (21.2.1b)$$

A pure-*C* Hamiltonian $\mathbf{H}^C$ with *A=D* belongs to C_2^C subgroup of *SU(2)* and conserves *angular momentum* l_3 which becomes a key observable and quantum label. In terms of **a**-operators, $\mathbf{H}^C$ is.

$$\mathbf{H}^C = A\left(\mathbf{a}_1^\dagger\mathbf{a}_1+\mathbf{a}_2^\dagger\mathbf{a}_2+\mathbf{1}\right)+iC\left(\mathbf{a}_2^\dagger\mathbf{a}_1-\mathbf{a}_1^\dagger\mathbf{a}_2\right) \qquad (21.2.2)$$

From (21.1.22) it appears that the eigenvalues will be the same as (21.1.25) but with Ω = *2C*. This will be shown below when the eigenstates are derived. The fundamental representation (21.1.16) of $\mathbf{H}^C$ is

$$\left\langle \mathbf{H}^{C} \right\rangle_{\upsilon=1}^{Fundamental} = \begin{array}{c|cc} n_1,n_2 & |1,0\rangle & |0,1\rangle \\ \hline \langle 1,0| & A & -iC \\ \langle 0,1| & +iC & A \end{array} + A\mathbf{1} \qquad (21.2.3)$$

$\mathbf{H}^C$ commutes with a complex reflection σ_C and a real continuous rotation $\mathbf{R}[\phi]$ generated by σ_C.

$$s_C = \begin{pmatrix} 0 & -i \\ i & 0 \end{pmatrix} \quad , \quad \mathbf{R}[\phi] = \begin{pmatrix} \cos\phi & -\sin\phi \\ \sin\phi & \cos\phi \end{pmatrix} = e^{-i\phi s_C} \qquad (21.2.4)$$

This means $\mathbf{H}^C$ is "smooth" or perfectly circular. It does not have any potential valleys or "bumps" which change angular momentum and require standing-or-galloping-wave eigenstates. So its eigenwaves (like those of a Ring Laser) have no nodes or antinodes and are of the form $e^{\pm im\phi} = (x_1 \pm i x_2)^m$ for which the probability distribution is perfectly circular in the complex phasor plane. Their complex continuous circularity provides some more mnemonic reasons to use the letter *"C"* to designate such a symmetry.

The complex *C*-symmetry $(x_1 \pm i x_2)$-states differ from the real standing wave (x_1 and x_2) states of $C_2{}^A$ symmetry or ($x_1 \pm x_2$) states of $C_2{}^B$ symmetry described in Sec. 10.2(a) through Sec. 10.3(b). We started by basing our oscillator theory on linear (x_1 and x_2) states of $C_2{}^A$. The *A*-axis bases will need to be moved to the chiral *C*-axis of Fig. 10.5.6 using, for example, a *90°* rotation around the *B*-axis. This will be done shortly.

(1) Angular momentum labeling: Fundamental base states $\{|\uparrow\rangle, |\downarrow\rangle\}$

First, let us re-label and "rename" the lowest five *U(2)* base sets as follows.

$$\left|\begin{smallmatrix} j \\ m \end{smallmatrix}\right\rangle = |n_1 n_2\rangle \quad \left\{ \begin{array}{lll} j=0 & \left|\begin{smallmatrix} 0 \\ 0 \end{smallmatrix}\right\rangle = |00\rangle & \text{"scalar"} \\ \hline j=\frac{1}{2} & \left|\begin{smallmatrix} 1/2 \\ 1/2 \end{smallmatrix}\right\rangle = |10\rangle = |\uparrow\rangle & \text{"spinor"} \\ & \left|\begin{smallmatrix} 1/2 \\ -1/2 \end{smallmatrix}\right\rangle = |01\rangle = |\downarrow\rangle & \\ \hline j=1 & \left|\begin{smallmatrix} 1 \\ 1 \end{smallmatrix}\right\rangle = |20\rangle & \\ & \left|\begin{smallmatrix} 1 \\ 0 \end{smallmatrix}\right\rangle = |11\rangle & \text{"3-vector"} \\ & \left|\begin{smallmatrix} 1 \\ -1 \end{smallmatrix}\right\rangle = |02\rangle & \\ \hline j=\frac{3}{2} & \left|\begin{smallmatrix} 3/2 \\ 1/2 \end{smallmatrix}\right\rangle = |30\rangle & \\ & \left|\begin{smallmatrix} 3/2 \\ 1/2 \end{smallmatrix}\right\rangle = |21\rangle & \text{"4-spinor"} \\ & \left|\begin{smallmatrix} 3/2 \\ -1/2 \end{smallmatrix}\right\rangle = |12\rangle & \\ & \left|\begin{smallmatrix} 3/2 \\ -3/2 \end{smallmatrix}\right\rangle = |03\rangle & \\ \hline j=2 & \left|\begin{smallmatrix} 2 \\ 2 \end{smallmatrix}\right\rangle = |40\rangle & \\ & \left|\begin{smallmatrix} 2 \\ 1 \end{smallmatrix}\right\rangle = |31\rangle & \\ & \left|\begin{smallmatrix} 2 \\ 0 \end{smallmatrix}\right\rangle = |22\rangle & \text{"tensor"} \\ & \left|\begin{smallmatrix} 2 \\ -1 \end{smallmatrix}\right\rangle = |13\rangle & \\ & \left|\begin{smallmatrix} 2 \\ -2 \end{smallmatrix}\right\rangle = |04\rangle & \\ \hline \vdots & & \end{array} \right. \quad \left\{ \begin{array}{ll} j = \frac{\upsilon}{2} = \frac{n_1+n_2}{2} & n_1 = j+m = 2\upsilon+m \\ m = \frac{n_1-n_2}{2} & n_2 = j-m = 2\upsilon-m \end{array} \right. \qquad (21.2.5)$$

Famous examples of chiral spin objects include electrons, nucleons, neutrinos, and other particles of total spin *j=1/2* units of ħ. If we choose the fundamental *U(2)* bases states {|1⟩,|2⟩} to be *spin-up* |↑⟩ and *spin-dn* |↓⟩ then the quantum theory of angular momentum is mathematically identical to an analysis *U(2)* oscillator states. Each number-1 boson counts for one-half ħ-unit of angular momentum *m =+1/2* while each number-2 boson counts for minus one-half ħ-unit of angular momentum *m =-1/2* along the *C*-axis or *Z*-axis.

U(2) levels from Fig. 21.1.1 are separated and labeled according to angular momentum notation in Fig. 21.2.1. *Odd*-υ and half-integral *j= 1/2, 3/2,.. levels* are sketched on the left-hand side while the *even*-υ and integral *j= 0, 1, 2,.. levels* are sketched on the right-hand side. Common names "*spinor*", "*vector*" and "*tensor*" are applied to multiplets *j=1/2, 1,* and *2*, respectively. The half-integral-*j* side is generally associated with the group *U(2)* that works on complex *2*-dimensional "spinor" space, while the integral-*j* side (which belongs to *U(2)*, too) is generally associated with real *3*-dimensional *R(3)* rotations in optical *ABC*-space or in a real *XYZ*-space, not entirely different from the one in which we live.

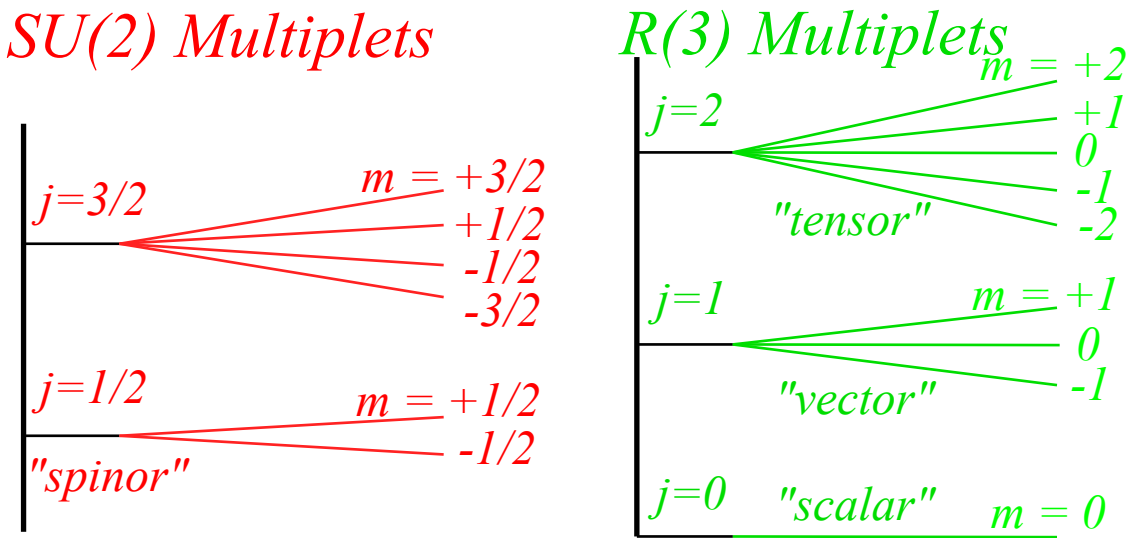

Fig. 21.2.1 SU(2) and R(3) angular momentum levels labeled by j and m.

A *C*-Hamiltonian is diagonalized by a Θ=*90°* rotation around the *X* or *B*-axis which takes a spin vector **S** on the *Z* or *A*-axis down to the *Y* or *C*-axis. *X*-rotations have polar angles [φ =*0°*, ϑ =*90°*]. Putting these angles into a Darboux rotation matrix (2.10.15d) gives

$$\langle \mathbf{R}_B(90°)\rangle = \langle \mathbf{R}[\varphi = 0°, \vartheta = 90°, \Theta = 90°]\rangle = \begin{pmatrix} \frac{1}{\sqrt{2}} & \frac{-i}{\sqrt{2}} \\ \frac{-i}{\sqrt{2}} & \frac{1}{\sqrt{2}} \end{pmatrix} = \begin{pmatrix} \langle R|x_1\rangle & \langle R|x_2\rangle \\ \langle L|x_1\rangle & \langle L|x_2\rangle \end{pmatrix} \qquad (21.2.6a)$$

This is a transformation between linear optical polarization states {|x_1⟩,|x_2⟩} and states of circular right-or-left-polarization {|*R*⟩,|*L*⟩} or electronic states of spin-up-or-dn {|↑⟩= |+$^1/_2$⟩,|↓⟩= |–$^1/_2$⟩}

$$|R\rangle=|\uparrow\rangle=\left|\begin{matrix}1/2\\+1/2\end{matrix}\right\rangle=\frac{|x_1\rangle+i|x_2\rangle}{\sqrt{2}},\qquad |L\rangle=|\downarrow\rangle=\left|\begin{matrix}1/2\\-1/2\end{matrix}\right\rangle=\frac{i|x_1\rangle+|x_2\rangle}{\sqrt{2}},$$
$$\langle R|=\langle\uparrow|=\left\langle\begin{matrix}1/2\\+1/2\end{matrix}\right|=\frac{\langle x_1|-i\langle x_2|}{\sqrt{2}},\qquad \langle L|=\langle\downarrow|=\left\langle\begin{matrix}1/2\\-1/2\end{matrix}\right|=\frac{-i\langle x_1|+\langle x_2|}{\sqrt{2}}. \tag{21.2.6b}$$

This must also be the transformation between the corresponding sets of $\{\mathbf{a}^\dagger_1,\mathbf{a}^\dagger_2\}$ and $\{\mathbf{a}^\dagger\uparrow,\mathbf{a}^\dagger\downarrow\}$ operators which create the base states $\{|x_1\rangle=\mathbf{a}^\dagger_1|0\rangle,|x_2\rangle=\mathbf{a}^\dagger_2|0\rangle\}$ and $\{|\uparrow\rangle=\mathbf{a}^\dagger\uparrow|0\rangle,|\downarrow\rangle=\mathbf{a}^\dagger\downarrow|0\rangle\}$.

$$\mathbf{a}^\dagger_R=\mathbf{a}^\dagger_\uparrow=\mathbf{a}^\dagger_{+1/2}=\frac{\mathbf{a}^\dagger_1+i\mathbf{a}^\dagger_2}{\sqrt{2}},\qquad \mathbf{a}^\dagger_L=\mathbf{a}^\dagger_\downarrow=\mathbf{a}^\dagger_{-1/2}=\frac{i\mathbf{a}^\dagger_1+\mathbf{a}^\dagger_2}{\sqrt{2}},$$
$$\mathbf{a}_R=\mathbf{a}_\uparrow=\mathbf{a}_{+1/2}=\frac{\mathbf{a}_1-i\mathbf{a}_2}{\sqrt{2}},\qquad \mathbf{a}_L=\mathbf{a}_\downarrow=\mathbf{a}_{-1/2}=\frac{-i\mathbf{a}^\dagger_1+\mathbf{a}^\dagger_2}{\sqrt{2}}. \tag{21.2.6c}$$

It does indeed diagonalize the fundamental ($\upsilon=1$) or ($j=1/2$) **H**-submatrix (21.1.16) for $C_2{}^C$ symmetry.

$$\begin{pmatrix}\langle\uparrow|x_1\rangle & \langle\uparrow|x_2\rangle\\ \langle\downarrow|x_1\rangle & \langle\downarrow|x_2\rangle\end{pmatrix}\cdot\begin{pmatrix}\langle x_1|\mathbf{H}|x_1\rangle & \langle x_1|\mathbf{H}|x_2\rangle\\ \langle x_2|\mathbf{H}|x_1\rangle & \langle x_2|\mathbf{H}|x_2\rangle\end{pmatrix}\cdot\begin{pmatrix}\langle x_1|\uparrow\rangle & \langle x_1|\downarrow\rangle\\ \langle x_2|\uparrow\rangle & \langle x_2|\downarrow\rangle\end{pmatrix}=\begin{pmatrix}\langle\uparrow|\mathbf{H}|\uparrow\rangle & \langle\uparrow|\mathbf{H}|x_2\rangle\\ \langle\downarrow|\mathbf{H}|\uparrow\rangle & \langle\downarrow|\mathbf{H}|\downarrow\rangle\end{pmatrix}$$
$$\begin{pmatrix}\frac{1}{\sqrt{2}} & \frac{-i}{\sqrt{2}}\\ \frac{-i}{\sqrt{2}} & \frac{1}{\sqrt{2}}\end{pmatrix}\cdot\begin{pmatrix}0 & -iC\\ iC & 0\end{pmatrix}\cdot\begin{pmatrix}\frac{1}{\sqrt{2}} & \frac{-i}{\sqrt{2}}\\ \frac{-i}{\sqrt{2}} & \frac{1}{\sqrt{2}}\end{pmatrix}=\begin{pmatrix}C & 0\\ 0 & -C\end{pmatrix} \tag{21.2.6d}$$

The resulting wave functions are a complex-conjugate pair of two-dimensional Gaussians.

$$\psi_{1_\uparrow 0_\downarrow}(x_1,x_2)=\frac{\sqrt{2}(x_1+ix_2)e^{-\left(x_1^2+x_2^2\right)/2}}{(\pi)^{1/2}},\ \psi_{0_\uparrow 1_\downarrow}(x_1,x_2)=\frac{\sqrt{2}(x_1-ix_2)e^{-\left(x_1^2+x_2^2\right)/2}}{(\pi)^{1/2}} \tag{21.2.7}$$

The two have identical probability distribution which is plotted in Fig. 21.2.2. (Also, recall Fig. 21.1.6.)

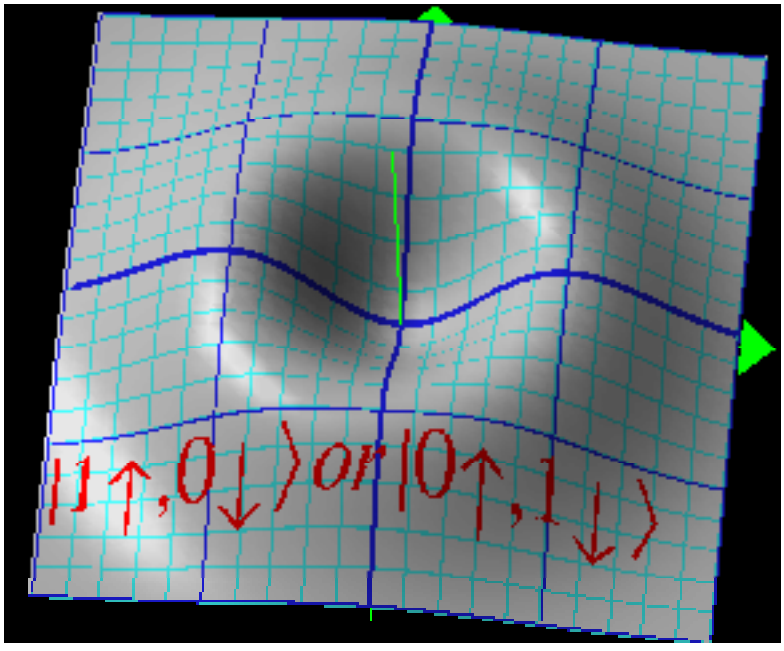

Fig. 21.2.2 2-D Oscillator probability distributions: $|\Psi_{1\uparrow 0\downarrow}(x_1,x_2)|^2$ or $|\Psi_{0\uparrow 1\downarrow}(x_1,x_2)|^2$.

Notice how the probability drops to zero quickly near the origin. This is a general property of an eigentate with non-zero momentum ℓ in ℓ -conserving systems. As a particle approaches the origin with non-zero angular momentum, it gains speed and kinetic energy without limit, like a dust particle in a perfect vortex. However, if energy is also conserved then particles simply must avoid the origin.

(2) 3-Vector base states (υ=2) or (j=1)

The preceding procedures may be used to find the eigenvectors of the excited (υ=*2, 3, 4...*) **H**-sub-matrices. For example, the (υ=*2*) or (*j=1*) eigenvectors of a $C_2{}^C$ symmetric **H** must be the following.

$$\begin{aligned}
|2_\uparrow 0_\downarrow\rangle &= \frac{\mathbf{a}_\uparrow^{\dagger 2}}{\sqrt{2!}}|0\rangle = \frac{\left(\mathbf{a}_1^\dagger + i\mathbf{a}_2^\dagger\right)^2}{2\sqrt{2!}}|0\rangle = \frac{\mathbf{a}_1^{\dagger 2} + 2i\mathbf{a}_1^\dagger\mathbf{a}_2^\dagger - \mathbf{a}_2^{\dagger 2}}{2\sqrt{2}}|0\rangle = \frac{1}{2}|2_1 0_2\rangle + \frac{i}{\sqrt{2}}|1_1 1_2\rangle - \frac{1}{2}|0_1 2_2\rangle \\
|1_\uparrow 1_\downarrow\rangle &= \frac{\mathbf{a}_\uparrow^\dagger \mathbf{a}_\downarrow^\dagger}{\sqrt{1!}\sqrt{1!}}|0\rangle = \frac{\left(\mathbf{a}_1^\dagger + i\mathbf{a}_2^\dagger\right)\left(\mathbf{a}_1^\dagger - i\mathbf{a}_2^\dagger\right)}{2}|0\rangle = \frac{\mathbf{a}_1^{\dagger 2} + \mathbf{a}_2^{\dagger 2}}{2}|0\rangle = \frac{1}{\sqrt{2}}|2_1 0_2\rangle + \frac{1}{\sqrt{2}}|0_1 2_2\rangle \\
|0_\uparrow 2_\downarrow\rangle &= \frac{\mathbf{a}_\downarrow^{\dagger 2}}{\sqrt{2!}}|0\rangle = \frac{\left(\mathbf{a}_1^\dagger - i\mathbf{a}_2^\dagger\right)^2}{2\sqrt{2!}}|0\rangle = \frac{\mathbf{a}_1^{\dagger 2} - 2i\mathbf{a}_1^\dagger\mathbf{a}_2^\dagger - \mathbf{a}_2^{\dagger 2}}{2\sqrt{2}}|0\rangle = \frac{1}{2}|2_1 0_2\rangle - \frac{i}{\sqrt{2}}|1_1 1_2\rangle - \frac{1}{2}|0_1 2_2\rangle
\end{aligned} \qquad (21.2.8)$$

We verify that the resulting vectors are eigenvectors of the 3-by-3 submatrix of (21.1.15c).

$$\begin{aligned}
&(j = \upsilon/2 = 1)\ \textit{Eigenvalues}: \quad 2C \quad , \quad 0 \quad , \quad -2C \\
&\begin{pmatrix} \cdot & -iC\sqrt{2} & \cdot \\ iC\sqrt{2} & \cdot & -iC\sqrt{2} \\ \cdot & iC\sqrt{2} & \cdot \end{pmatrix} \cdot \begin{pmatrix} 1/2 \\ i/\sqrt{2} \\ -1/2 \end{pmatrix}, \begin{pmatrix} 1/\sqrt{2} \\ 0 \\ 1/\sqrt{2} \end{pmatrix}, \begin{pmatrix} 1/2 \\ -i/\sqrt{2} \\ -1/2 \end{pmatrix}
\end{aligned} \qquad (21.2.9)$$

The splitting between neighboring levels is $\Omega = 2C$ as required by (21.1.22)

The (υ=2) eigenfunctions $\langle x_1\, x_2|n_1\, n_2\rangle$ in the *A*-basis are products of 1-D waves (20.3.40).

$$\psi_{2_1 0_1}(x_1,x_2) = \langle x_1|2\rangle\langle x_2|0\rangle \ , \quad \psi_{1_1 1_1}(x_1,x_2) = \langle x_1|1\rangle\langle x_2|1\rangle \ , \quad \psi_{1_1 1_1}(x_1,x_2) = \langle x_1|0\rangle\langle x_2|2\rangle$$

$$= Ne^{-\left(x_1^2+x_2^2\right)/2}\sqrt{2}\left(x_1^2 - \frac{1}{2}\right), \quad = Ne^{-\left(x_1^2+x_2^2\right)/2}2\left(x_1 x_2\right), \quad = Ne^{-\left(x_1^2+x_2^2\right)/2}\sqrt{2}\left(x_2^2 - \frac{1}{2}\right)$$

(21.2.10a) (21.2.10b) (21.2.10c)

Combining them according to (21.2.8) gives the (υ=2) eigenwaves for a *C*-type Hamiltonian.

$$\psi_{2_\uparrow 0_\downarrow} = \frac{1}{2}\psi_{2_1 0_1} + \frac{i\sqrt{2}}{2}\psi_{1_1 1_1} - \frac{1}{2}\psi_{0_1 1_1} = Ne^{-\frac{r^2}{2}}\frac{x_1^2 + 2ix_1 x_2 - x_2^2}{\sqrt{2}} = Ne^{-\frac{r^2}{2}}\frac{\left(x_1 + ix_2\right)^2}{\sqrt{2}} \qquad (21.2.10d)$$

$$\psi_{1_\uparrow 1_\downarrow} = \frac{1}{\sqrt{2}}\psi_{2_1 0_1} + \frac{1}{\sqrt{2}}\psi_{0_1 1_1} = Ne^{-\frac{r^2}{2}}\frac{\sqrt{2}\left(x_1^2 + x_2^2 - 1\right)}{\sqrt{2}} = Ne^{-\frac{r^2}{2}}\left(x_1^2 + x_2^2 - 1\right) \qquad (21.2.10e)$$

$$\psi_{0_\uparrow 2_\downarrow} = \frac{1}{2}\psi_{2_1 0_1} - \frac{i\sqrt{2}}{2}\psi_{1_1 1_1} - \frac{1}{2}\psi_{0_1 1_1} = Ne^{-\frac{r^2}{2}}\frac{x_1^2 + 2ix_1 x_2 - x_2^2}{\sqrt{2}} = Ne^{-\frac{r^2}{2}}\frac{\left(x_1 - ix_2\right)^2}{\sqrt{2}} \qquad (21.2.10f)$$

The *A*-type waves $\psi_{2_1 0_2}$ and $\psi_{1_1 1_2}$ plotted in Fig. 21.2.3 have lumps and bumps that are aligned to Cartesian $(x_1\, x_2)$ coordinates.

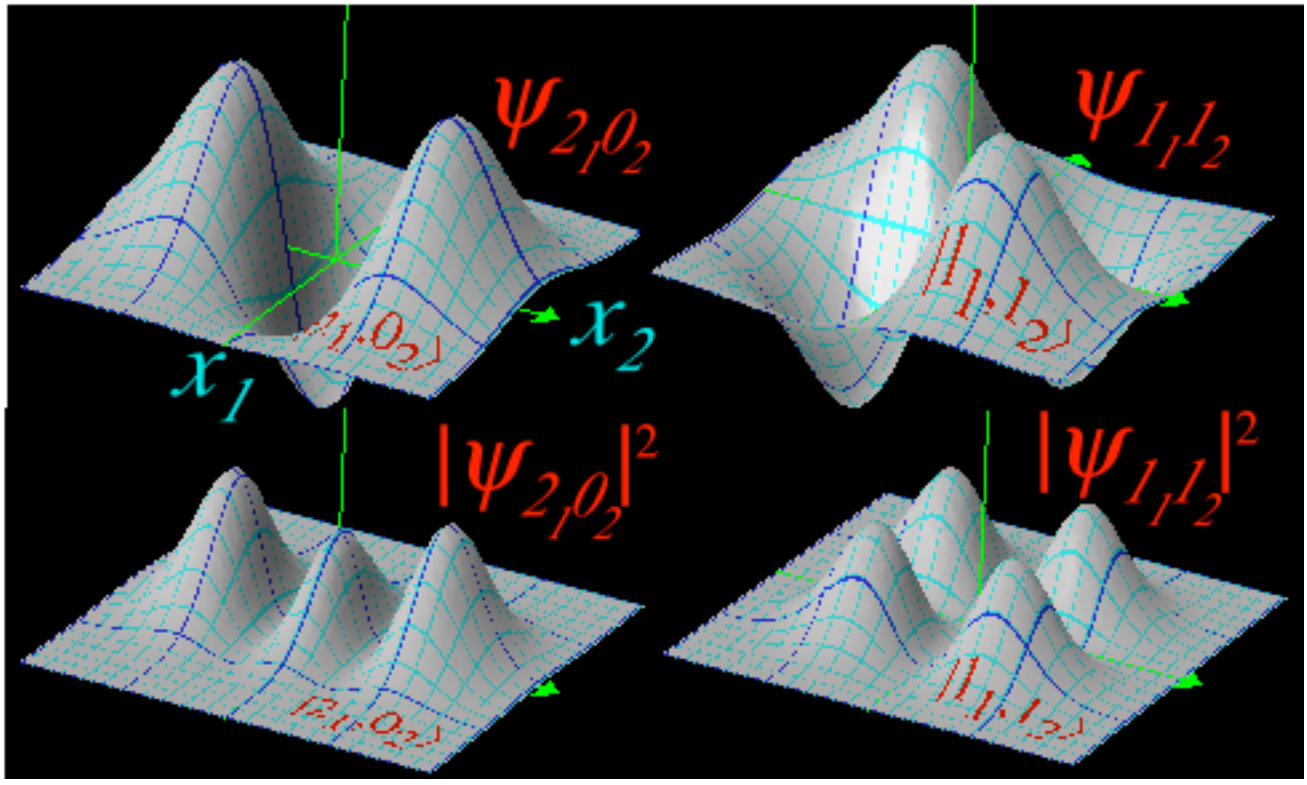

Fig. 21.2.3 (υ=2) Type-A standing waves and distributions: $|\Psi_{2_1 0_2}(x_1,x_2)|^2$ *and* $|\Psi_{1_1 1_2}(x_1,x_2)|^2$.

In contrast, the *C*-type waves $\psi_{2\uparrow 0\downarrow}$ and $\psi_{1\uparrow 1\downarrow}$ plotted in Fig. 21.2.4 are waves moving around in circular orbits with vibrational angular momentum of ±2 and 0.

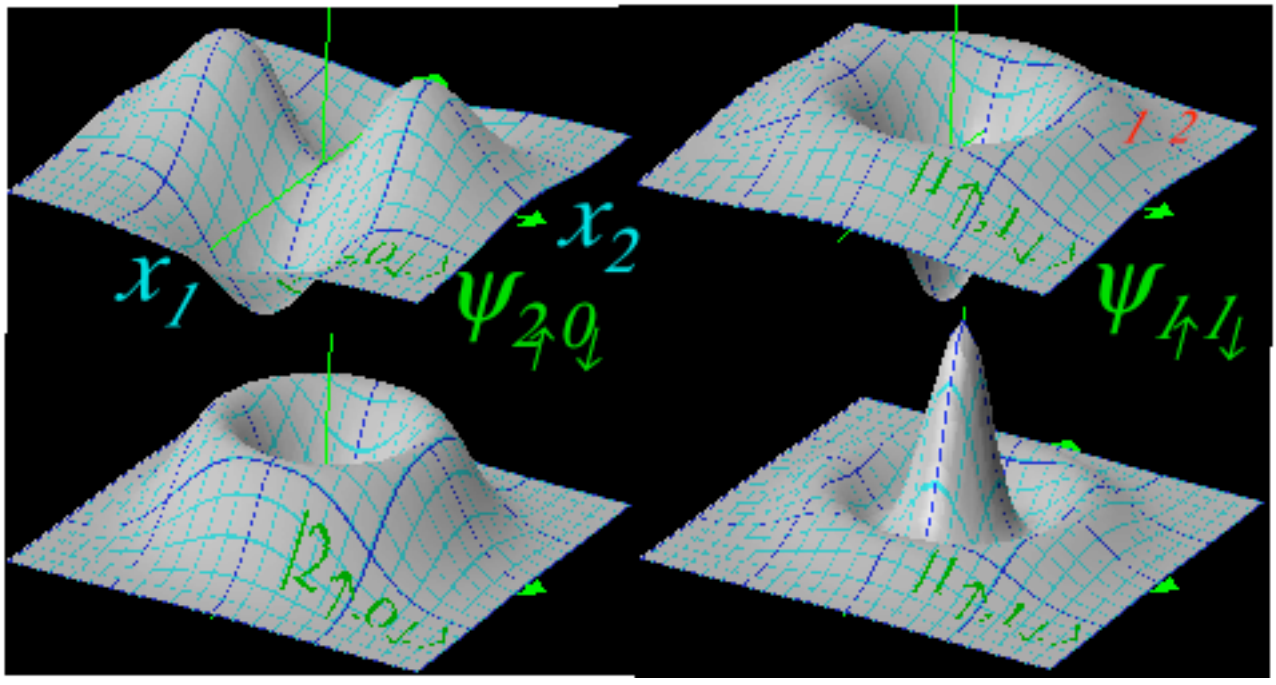

Fig. 21.2.4 (υ=2) Type-C moving waves and distributions: $|\Psi_{2\uparrow 0\downarrow}(x_1,x_2)|^2$ *and* $|\Psi_{1\uparrow 1\downarrow}(x_1,x_2)|^2$.
The angular momentum structure can be seen by rewriting the wavefunctions in polar coordinates.

$$\psi_{2_\uparrow 0_\downarrow} = Ne^{-\frac{r^2}{2}} \frac{\left(x_1 + ix_2\right)^2}{\sqrt{2}} = \psi_{2m=2}^{2j=2} = Ne^{-\frac{r^2}{2}} \frac{r^2 e^{i2\theta}}{\sqrt{2}} \qquad (21.2.10d)$$

$$\psi_{1_\uparrow 1_\downarrow} = Ne^{-\frac{r^2}{2}} \left(x_1^2 + x_2^2 - 1\right) = \psi_{2m=0}^{2j=2} = Ne^{-\frac{r^2}{2}} \left(r^2 - 1\right) e^{i0\theta} \qquad (21.2.10d)$$

$$\psi_{0_\uparrow 2_\downarrow} = Ne^{-\frac{r^2}{2}} \frac{\left(x_1 - ix_2\right)^2}{\sqrt{2}} = \psi_{2m=-2}^{2j=2} = Ne^{-\frac{r^2}{2}} \frac{r^2 e^{-i2\theta}}{\sqrt{2}} \qquad (21.2.10d)$$

Quantum numbers for *C*-type vibrational states are the *radial quantum number (υ=2j)* and the *vibrational angular momentum quantum number* μ.

$$\upsilon = 2j = n\uparrow + n\downarrow \quad , \quad \mu = 2m = n\uparrow - n\downarrow \qquad (21.2.11)$$

A *C*-type vibrational eigenstate has μ angular waves and 2μ angular moving wave zeros (two for each wave). For larger angular momentum the wave tends to avoid the origin more and more as shown in Fig. 21.2.5 below in a comparison between a μ=*1* and a μ=*4* probability distribution.

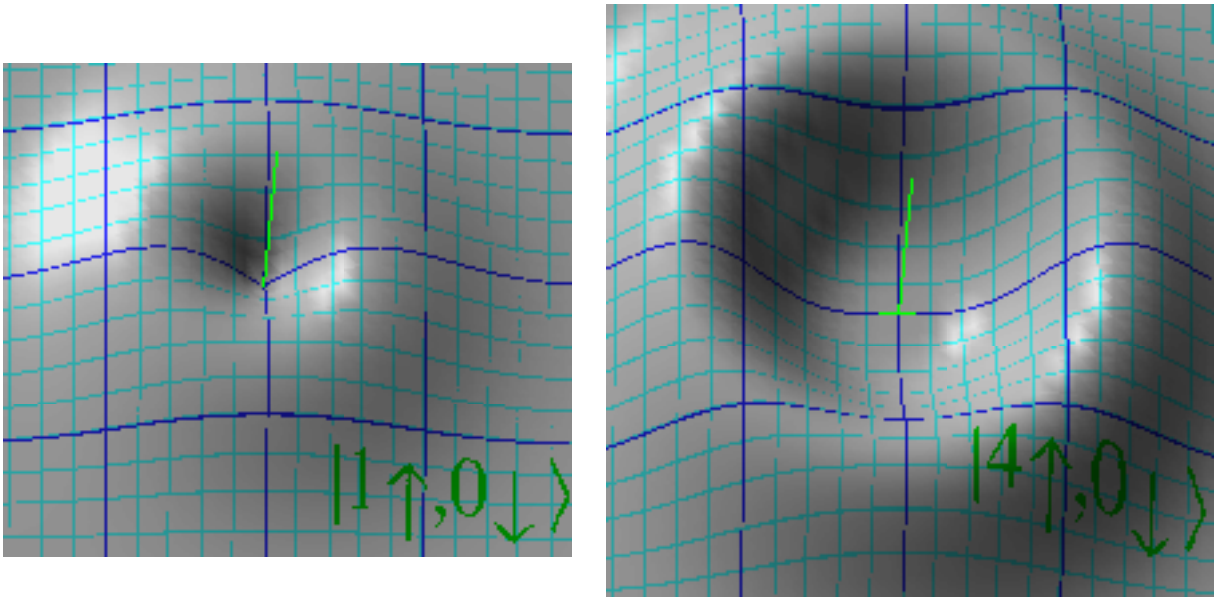

Fig. 21.2.5 (υ=2) Type-C moving wave distributions: $|\Psi_{1\uparrow 0\downarrow}(x_1,x_2)|^2$ *and* $|\Psi_{4\uparrow 0\downarrow}(x_1,x_2)|^2$.

As the azimuthal angualr momentum quantum number μ=*2m* increases, the location of the circular orbital radius becomes more and more clearly defined.

(b) Polar coordinates: C_2^C symmetry variable separation

An alternative (and historically much older) way to obtain *C*-symmetry eigenfunctions is to use coordinates based on circular symmetry, namely, polar coordinates (r,ϕ) instead of Cartesian (x,y) or

$$x = x_1 = r\cos\phi\ , \qquad y = x_2 = r\sin\phi\ . \tag{21.2.12}$$

The Jacobian transformation between the Cartesian and polar coordinates relates their derivatives.

$$\begin{pmatrix} \frac{\partial}{\partial r} \\ \frac{\partial}{\partial \phi} \end{pmatrix} = \begin{pmatrix} \frac{\partial x}{\partial r} & \frac{\partial y}{\partial r} \\ \frac{\partial x}{\partial \phi} & \frac{\partial y}{\partial \phi} \end{pmatrix} \begin{pmatrix} \frac{\partial}{\partial x} \\ \frac{\partial}{\partial y} \end{pmatrix} = \begin{pmatrix} \cos\phi & \sin\phi \\ -r\sin\phi & r\cos\phi \end{pmatrix} \begin{pmatrix} \frac{\partial}{\partial x} \\ \frac{\partial}{\partial y} \end{pmatrix} \tag{21.2.13a}$$

The inverse (Kajobian) transformation lets us rewrite the Cartesian Schrodinger equation.

$$\begin{pmatrix} \frac{\partial}{\partial x} \\ \frac{\partial}{\partial y} \end{pmatrix} = \begin{pmatrix} \frac{\partial r}{\partial x} & \frac{\partial \phi}{\partial x} \\ \frac{\partial r}{\partial y} & \frac{\partial \phi}{\partial y} \end{pmatrix} \begin{pmatrix} \frac{\partial}{\partial r} \\ \frac{\partial}{\partial \phi} \end{pmatrix} = \begin{pmatrix} \cos\phi & -\frac{1}{r}\sin\phi \\ \sin\phi & \frac{1}{r}\cos\phi \end{pmatrix} \begin{pmatrix} \frac{\partial}{\partial r} \\ \frac{\partial}{\partial \phi} \end{pmatrix} \tag{21.2.13b}$$

The oscillator Schrodinger equation in Cartesian coordinates

$$\frac{\partial^2\Psi}{\partial x^2} + \frac{\partial^2\Psi}{\partial y^2} - \frac{2M}{\hbar^2}\left(\frac{M\omega^2}{2}\left(x^2+y^2\right) - E\right)\Psi = 0\ , \tag{21.2.14a}$$

is rewritten as follows in polar coordinates.

$$\frac{\partial^2\Psi}{\partial r^2} + \frac{1}{r}\frac{\partial\Psi}{\partial r} + \frac{1}{r^2}\frac{\partial^2\Psi}{\partial\phi^2} - \frac{2M}{\hbar^2}\left(\frac{M\omega^2}{2}r^2 - E\right)\Psi = 0$$

(21.2.14a)

Separation of coordinate variables r and ϕ into a wavefunction $\Psi(r,\phi)=R(r)\varphi(\phi)$ is similar to the separation $\Psi(x,y)=\psi_x(x)\psi_y(y)$ for Cartesian coordinates and results in the following equation separation.

$$\frac{r^2}{R}\left[\frac{d^2R}{dr^2} + \frac{1}{r}\frac{dR}{dr}\right] - \frac{2Mr^2}{\hbar^2}\left(\frac{M\omega^2}{2}r^2 - E\right) = -\frac{1}{\varphi}\frac{\partial^2\varphi}{\partial\phi^2} = const. = m^2 \tag{21.2.15a}$$

Equality of the two ordinary equations of independent r and ϕ implies both equal a constant. Azimuthal symmetry and boundary conditions $\varphi(\phi)=\varphi(\phi\pm 2\pi)$ force m-quantization, so the constant is the square of azimuthal angular momentum quantum number $m=0,\pm1,\pm2..$.

$$\frac{\partial^2\varphi}{\partial\phi^2} = -m^2\varphi \qquad \text{or:} \qquad \varphi(\phi) = Ae^{im\phi} + Be^{-im\phi} \tag{21.2.15b}$$

The radial equation involves the constant m^2 in a more complicated way.

$$\frac{d^2R}{dr^2} + \frac{1}{r}\frac{dR}{dr} - \left[\frac{M^2\omega^2}{\hbar^2}r^2 + \frac{2M}{\hbar^2}E - \frac{m^2}{r^2}\right]R = 0 \tag{21.2.15c}$$

C-symmetry makes the angular moving waves in the ϕ-direction independent of the radial wave except through the constant m^2. Such a constant is called a *separation constant*.

As in the 1-D case of (20.1.12) it helps to factor out a Gaussian scaling function $s(r)=e^{-\alpha r^2}$ such that the factor $\rho(r)$ in the radial wave $R(r)=s(r)\rho(r)$ is a simpler function and preferably an r polynomial.

$$R = \rho e^{-\alpha r^2}$$
$$R' = \left(\rho' - 2\alpha r\rho\right)e^{-\alpha r^2} \qquad (21.2.16)$$
$$R'' = \left(\rho'' - 4\alpha r\rho' + \left[4\alpha^2 r^2 - 2\alpha\right]\rho\right)e^{-\alpha r^2}$$

Dropping the Gaussian converts (21.2.15c) to an equation of similar form.

$$R'' + \frac{R'}{r} - \left[\frac{M^2\omega^2}{\hbar^2}r^2 - \frac{2M}{\hbar^2}E + \frac{m^2}{r^2}\right]R = 0$$

$$\rho'' + \left[\frac{1}{r} - 4\alpha r\right]\rho' + \left[\left(4\alpha^2 - \frac{M^2\omega^2}{\hbar^2}\right)r^2 + \frac{2M}{\hbar^2}E - 4\alpha - \frac{m^2}{r^2}\right]\rho = 0 \qquad (21.2.17a)$$

This simplifies if we use the same Gaussian parameter $\alpha = M\omega/2\hbar$ from (20.1.10b) and set $E = \hbar\omega\varepsilon$.

$$\rho'' + \left[\frac{1}{r} - 4\alpha r\right]\rho' + \left[4\alpha(\varepsilon - 1) - \frac{m^2}{r^2}\right]\rho = 0 = r^2\rho'' + \left[r - 4\alpha r^3\right]\rho' + \left[4\alpha(\varepsilon-1)r^2 - m^2\right]\rho \qquad (21.2.17b)$$

Now a polynomial analysis will work by expanding the radial wave and its derivatives. Let $\varepsilon\_ = \varepsilon - 1$.

$$\rho = a_0 + a_1 r + a_2 r^2 + a_3 r^3 + a_4 r^4 + \ldots = \sum_{k=0} a_k r^k$$
$$\rho' = a_1 + 2a_2 r + 3a_3 r^2 + 4a_4 r^4 + 5a_5 r^5 + \ldots = \sum_{k=1} k a_k r^{k-1} \qquad (21.2.18)$$
$$\rho'' = 2a_2 + 6a_3 r + 12a_3 r^2 + 20a_4 r^4 + 30a_5 r^5 + \ldots = \sum_{k=2} k(k-1)a_k r^{k-2}$$

Putting this into each term of the radial equation gives series whose grand sum must be zero.

$$-m^2\rho = -m^2 a_0 - m^2 a_1 r - m^2 a_2 r^2 - m^2 a_3 r^3 - m^2 a_4 r^4 + \ldots = \sum_{k=0} -m^2 a_k r^k$$
$$4\alpha\varepsilon\_ r^2\rho = 4\alpha\varepsilon\_ a_0 r^2 + 4\alpha\varepsilon\_ a_1 r^3 + 4\alpha\varepsilon\_ a_2 r^4 + \ldots = \sum_{k=2} 4\alpha\varepsilon\_ a_{k-2} r^k$$
$$r\rho' = a_1 r + 2a_2 r^2 + 3a_3 r^3 + 4a_4 r^4 + \ldots = \sum_{k=1} k a_k r^k$$
$$r^2\rho'' = 2a_2 r^2 + 6a_3 r^3 + 12a_4 r^4 + \ldots = \sum_{k=2} k(k-1)a_k r^k$$
$$-4\alpha\varepsilon\_ r^3\rho' = -4\alpha a_1 r^3 - 8\alpha a_2 r^4 + \ldots = \sum_{k=3} -4\alpha(k-2)a_{k-2} r^k$$

(21.2.19)

The sum of coefficients of each power lying in each column above must vanish. The *0*-column gives

$$m^2 a_0 = 0$$

This says that wave amplitude a_0 must vanish for all non-zero momentum m. We noted after Fig. 21.2.5 that orbiting particles avoid the origin. Consider the general column or power-k as listed on the right hand side above. Setting the sum of the k- coefficients to zero leads to a *recursion relation*.

$$\left[4\alpha\varepsilon\_ - 4\alpha(k-2)\right]a_{k-2} = -\left[k(k-1) + k - m^2\right]a_k \qquad (21.2.20a)$$

This may be used as a *bottom-up* relation or else as a *top-down* relation.

$$a_{k+2} = \frac{-4\alpha(\varepsilon_- - k)}{(k+2)^2 - m^2} a_k \ , \qquad a_{k-2} = \frac{m^2 - k^2}{4\alpha(\varepsilon_- - k + 2)} a_k \qquad (21.2.20b)$$

The first starts with bottom coefficient a_0 or a_1 and computes the higher ones. The other works down. The bottom-up relation leads to the *quantization condition*

$$\varepsilon_- = N = k_> \ , \qquad (21.2.20c)$$

for some integer *principal quantum number N* in order that the polynomial order is finite and the wave is bounded by the Gaussian. The top-down relation leads to a *centrifugal exclusion condition*

$$k_< = |m| \ , \qquad (21.2.20d)$$

which limits the lowest degree $k_<=m$ allowed by a given angular momentum m. High powers r^k are "center-fleeing" with low radial wave near $r=0$. Momentum magnitude is restricted between zero and N.

$$0 \le |m| \le N$$

The quantization condition agrees with the energy spectrum previously derived in (21.1.25).

$$\hbar\omega\varepsilon_- = \hbar\omega(\varepsilon - 1) = \hbar\omega N \ ,$$

where we use $E = \hbar\omega\varepsilon$ and $\varepsilon_- = \varepsilon - 1$ from (21.2.17).

$$E = \hbar\omega\varepsilon = \hbar\omega(N+1) \qquad (21.2.20e)$$

Note the principal quantum number N is the total quantum number υ defined previously in (21.1.25).

$$N = \upsilon = n_1 + n_2$$

The $N=2=\varepsilon_-$ wave for $m=0$ in (21.2.10b) follows from (21.2.20b)

$$a_2 = \frac{-4\alpha\varepsilon_-}{(2)^2 - 0^2} a_0 = -2\alpha a_0 = -\frac{M\omega}{\hbar} a_0 \qquad (21.2.21)$$

In units such that $M\omega/\hbar = 1$ or $\alpha = 1/2$ this agrees with (21.2.10b).

$$R(r) = a_0 (1 - r^2)$$

21.3 N-Dimensional Oscillator Levels

The quantum levels *(1,2,3,4,...,υ,...)* of a 1D oscillator are singlet levels (no degeneracy). However, an isotropic (*U(2)* symmetric) 2D oscillator has levels whose degeneracy $\ell = \upsilon$ equals the principal quantum number. $\upsilon = n_1 + n_2 = (1,2,3,4,...,\upsilon,...)$, as seen in Fig. 21.1.1.

The degeneracies of isotropic (*U(N)* symmetric) *N-D* oscillators increase more rapidly. For a U(3) symmetric 3D oscillator the degeneracy numbers are $\ell = (1,3,6,10,...,\upsilon(\upsilon+1)/2,...)$. These are known as *triangular numbers*. Here we consider ways to describe oscillator levels.

(a) Pascal triangle and U(N) degeneracy

There are some geometric ways to organize and label oscillator degeneracy. The first uses Pascal's triangle of binomial coefficients as shown in Fig. 21.3.1. Each Pascal number is the sum of the two numbers directly above it as shown in Fig. 21.3.1(a). Numbers along a given *N*-diagonal are the degeneracy ℓ for each quantum number υ listed along the opposing *(υ)*-diagonal. It's a binomial coefficient $C_\upsilon^n = \binom{n}{\upsilon}$ that means the number of combinations of *n* things taken υ at a time.

$$\ell = C_\upsilon^{N-1+\upsilon} = \binom{N-1+\upsilon}{\upsilon} = \frac{(N-1+\upsilon)!}{\upsilon!(N-1)!} = \binom{N-1+\upsilon}{N-1} \tag{23.1.1}$$

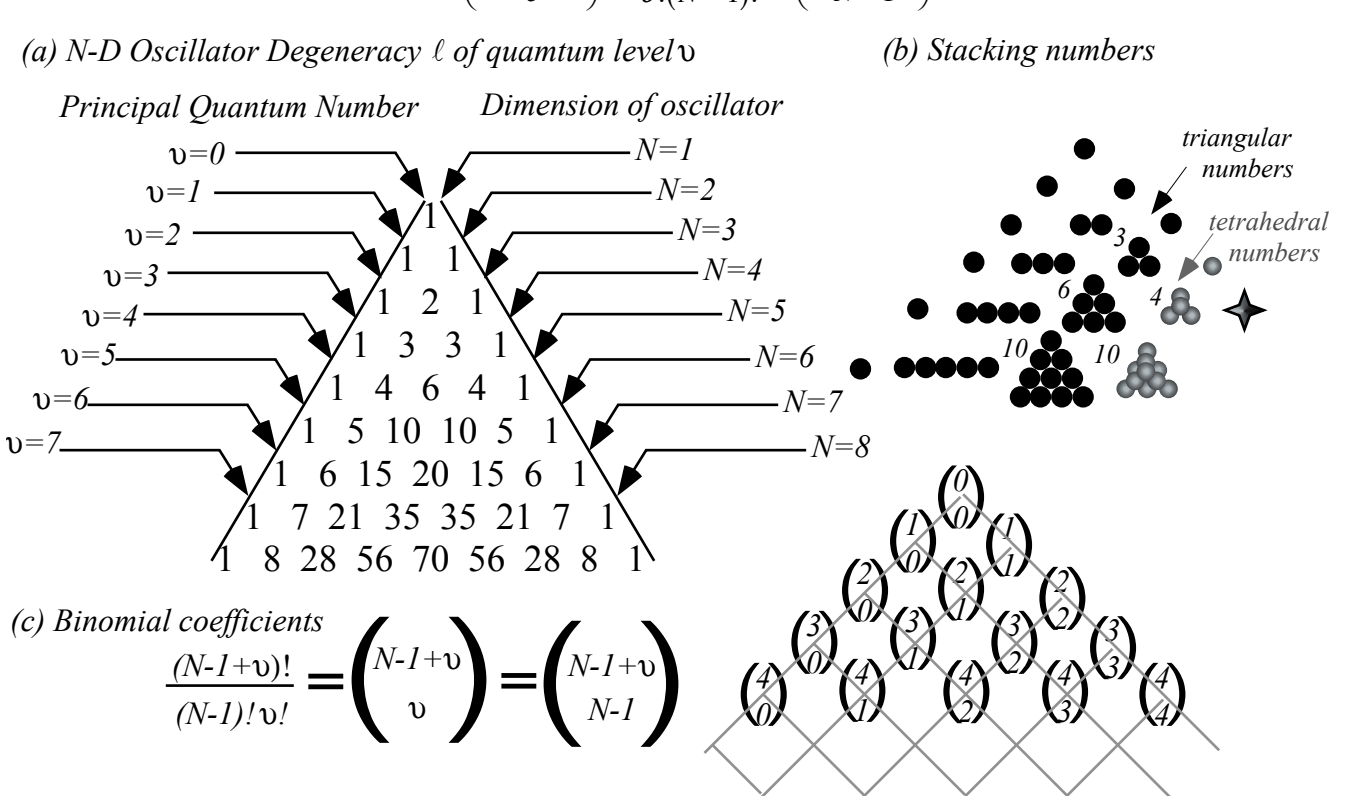

Fig. 21.3.1 Pascal binomial numbers related to oscillator level degeneracy.

The plot in Fig. 21.1.2 of the principal quantum number $\upsilon = n_1 + n_2$ versus individual *U(2)* oscillator quantum numbers n_1 and n_2 shows why Pascal's triangular numbers are relevant to oscillator degeneracy. An analogous plot of $\upsilon = n_1 + n_2 + n_3$ for a *U(3)* oscillator produces equilateral triangles stacked a diagonal distance $\upsilon = n_1 + n_2 + n_3$ from the corner of three Cartesian planes defining n_1 , n_2, and n_3 axes.

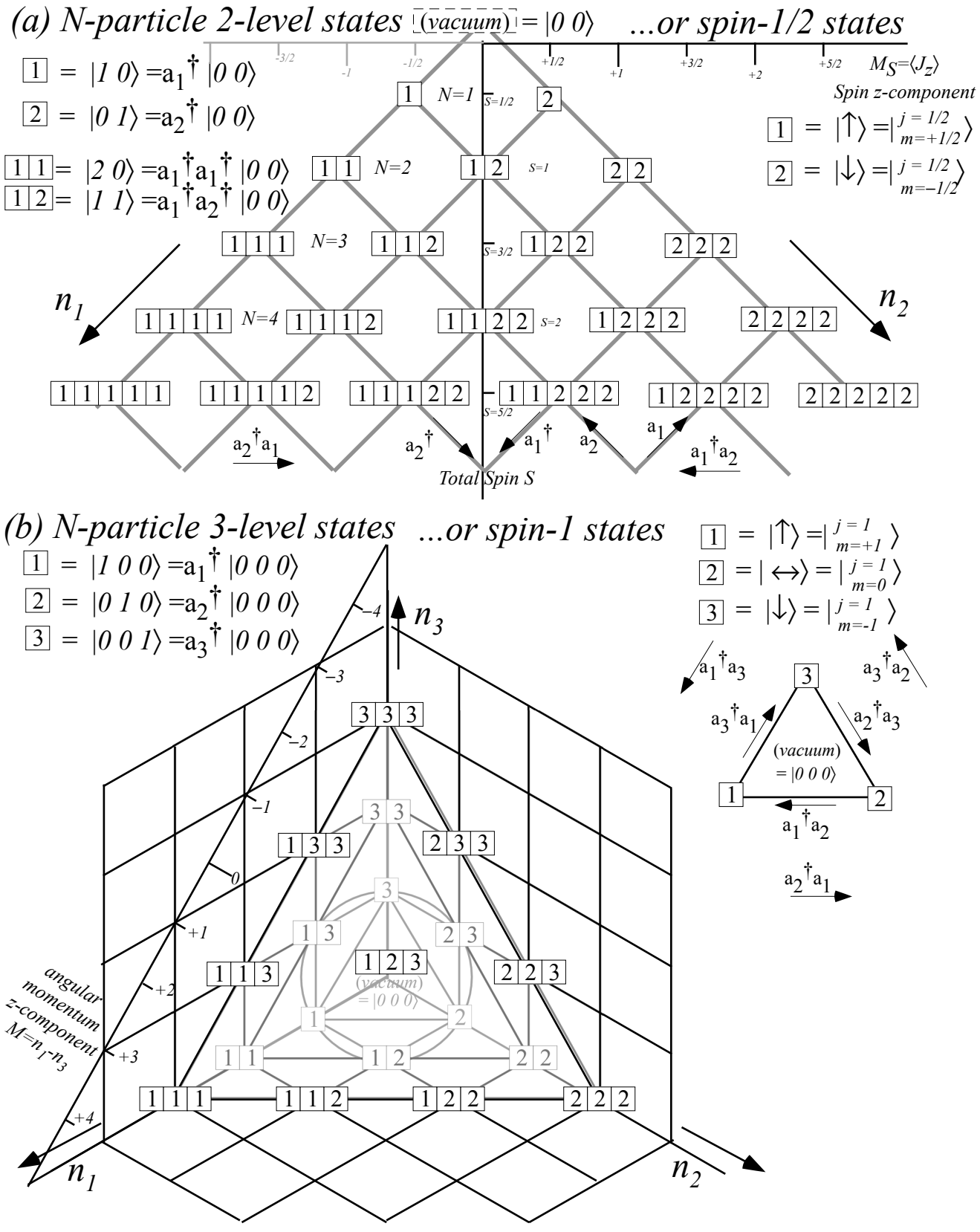

Fig. 21.3.2 N-quanta ("particle") multiplets (a) 2-Levels ("states") : Spin-1/2. (b) 3-Levels : Spin-1

Fig. 21.1.3(a) displays the 2D oscillator states in a way that is similar but upside down to Fig. 23.1.2(a). Each level has the same total number $N=\upsilon=n_1+n_2$ of quanta. We may think of each level as an N-particle state where by "particle" we mean a photon, vibron, libron, or any of a number of excitons that occupy our attention in modern physics. It is only important that each "X-on" or "Enr-on" may be created in arbitrary order, that is, has Bose symmetry as stated in (21.1.5) or again below.

$$[\,\mathbf{a}_m, \mathbf{a}_n] = \mathbf{a}_m\mathbf{a}_n - \mathbf{a}_n\mathbf{a}_m = \mathbf{0}\,, \quad [\,\mathbf{a}_m, \mathbf{a}^\dagger_n] = \mathbf{a}_m\mathbf{a}^\dagger_n - \mathbf{a}^\dagger_n\mathbf{a}_m = \delta_{mn}\mathbf{1}\,, \quad [\,\mathbf{a}^\dagger_m, \mathbf{a}^\dagger_n] = \mathbf{a}^\dagger_m\mathbf{a}^\dagger_n - \mathbf{a}^\dagger_n\mathbf{a}^\dagger_m = \mathbf{0}\,.$$

This is indicated by a *Young Tableaux* notation of boxes holding numbers that indicated the state or X-on numbers. Numbers may be permuted with in the rows without changing their meaning. Only the sum

$$N=S/2=\upsilon=n_1+n_2 \tag{21.3.2}$$

or difference

$$C=S_z/2=n_1-n_2 \tag{21.3.3}$$

Has physical significance. In the following Chapter 22, these numbers will define the photon "spin" that characterizes the intensity N and *one* of the polarization A, B, or C components in a quantum light beam. In Chapter 23, these quantum numbers will define total spin angular momentum S and its z-component S_z in the Schwinger development of rotational quanta.

Fig. 21.1.3(b) displays the 3D oscillator states in an analogous but 3-dimensional way with the 2D oscillator n_1-axis and n_2-axis lying on the floor of a Cartesian octant or "room" whose vertical n_3-axis is the number of quanta or "particles" in the 3rd oscillator state. Again any kind of "X-on" may use this geometry and the total number $N=\upsilon=n_1+n_2+n_3$ of these "particles" would be marked off on a *(1,1,1)*-axis coming straight out of this Fig. 21.3.2(b). With three dimensions or quanta n_1, n_2, and n_3 there are lots more ways that they can sum to a given N. That number is one of the triangular numbers *1,3,6,10*,.. listed in Pascal's triangle on the $N=3$ diagonal of Fig. 21.3.1(a) and indicated in Fig. 21.3.1(b). The triangles for $N=\upsilon=0, 1, 2$, and *3* are "stacked" in Fig. 21.3.2(b) with their Young tableaux state labeling.

These stacks make larger and larger tetrahedrons. Such tetrahedrons are just what are needed to make the next higher 4D-oscillator states whose degeneracy (for an isotropic oscillator) will be the tetrahedral numbers *1,4,10,15*.. listed in Fig. 21.3.1(b). These are the number of cannonballs in an N-sided stack seen sitting dissolutely in Civil War monuments throughout the educationally miasmic Southern states of a United States so tortured by its apparent need for that and other wars.

In contrast, there is much to learn about the quantum states by considering the geometry and algebra of these curious stacks and considering how it is that the idea of quantum *particles*, on one hand and quantum *states*, on the other, can be clearly defined in some cases and quite mixed up in others.

Problems for Chapter 21

From A to B

21.1.1. Consider a *B*-type 2D oscillator Hamiltonian:

$$\mathsf{H}^B = \frac{A}{2}\left(\mathsf{p}_1^2 + \mathsf{x}_1^2 + \mathsf{p}_2^2 + \mathsf{x}_2^2\right) + B\left(\mathsf{p}_1\mathsf{p}_2 + \mathsf{x}_1\mathsf{x}_2\right)$$

(a) Express it in terms of *A*-basis creation-destruction operators $\mathbf{a}_j = (\mathbf{x}_j + \mathrm{i}\,\mathbf{p}_j)/\sqrt{2}$ *(j=1,2)*.

(b) Compute its *A*-basis representation for the first five levels: *N=0, 1, 2, 3, 4,...*

(c) Plot the H^B eigenvalues for fixed *A=1* and varying between *B=-1* and *B=+1*.

(d) Diagonalize the representation for the three *N=2* levels and display the 3-by-3 trans-formation matrix $T_{B\leftarrow A}$ which effectively transforms from the *A*-basis to the *B*-basis. Does *T* depend on *A* or *B*?

Lines of degeneracy

21.1.2. The eigenvalues in Fig. 21.1.1 exhibit quite a number of degeneracy points as the splitting or beat frequency Ω varies relative to static oscillator frequency ω. Give a sketch of the algebra, geometry, or arithmetic that might shed some light on this. The revival crossings described in Ch. 9 might be relevant.

From B to C

21.1.3. Consider a *C*-type 2D oscillator Hamiltonian:

$$\mathsf{H}^C = \frac{A}{2}\left(\mathsf{p}_1^2 + \mathsf{x}_1^2 + \mathsf{p}_2^2 + \mathsf{x}_2^2\right) + C\left(\mathsf{x}_1\mathsf{p}_2 - \mathsf{x}_2\mathsf{p}_1\right)$$

(a) The *(N=2)*-transformation $T_{B\leftarrow A}$ from an *A*-basis to a *B*-basis derived in Exercise 21.1.1(d) might also be capable of continuing on from a *B*-basis to a *C*-basis. Does $T_{B\leftarrow A}$=$T_{C\leftarrow B}$? Check this. How is $T_{C\leftarrow A}$ related to these two?

(b) (For Ch. 23) How are these matrices related to the irreducible representations $D^{(1)}(\varphi,\vartheta,\Theta)$?

From 2 to 3

21.3.1. Using a ruler and a compass plot out the N-exciton states of a 3D isotropic harmonic oscillator for *N=3* and for *N=4* (as in Fig. 21.3.2(b). Label each plot with tableaux state labels.

(a) Show how the energy levels would split for *N= 1, 2, 3*, and *4* if oscillator-3 shifted up by 0.1 ω.

(b) Plot the 2D oscillator states (as in Fig. 21.3.2(a) that belong to each level that splits out.

To 4

21.3.2. How would you plot the states and their tableaux for a *four* dimensional (4D) oscillator?

(a) Do it for principal quantum number or "X-on" number *N= 1, 2,* and *3*.

(b) Show how the energy levels would split if oscillator-4 shifted up by 0.1 ω.